

Distribution Agreement

In presenting this thesis as a partial fulfillment of the requirements for a degree from Emory University, I hereby grant to Emory University and its agents the non-exclusive license to archive, make accessible, and display my thesis in whole or in part in all forms of media, now or hereafter now, including display on the World Wide Web. I understand that I may select some access restrictions as part of the online submission of this thesis. I retain all ownership rights to the copyright of the thesis. I also retain the right to use in future works (such as articles or books) all or part of this thesis.

Wenxiao Deng

April 12, 2021

Powering Polyvalent DNA Motors Using Exonuclease III

By

Wenxiao Deng

Khalid Salaita, Ph.D.

Adviser

Department of Chemistry

Dr. Khalid Salaita

Adviser

Dr. Vincent Conticello

Committee Member

Dr. Le Chen

Committee Member

2021

Powering Polyvalent DNA Motors Using Exonuclease III

By

Wenxiao Deng

Khalid Salaita, Ph.D.

Adviser

An abstract of
a thesis submitted to the Faculty of Emory College of Arts and Sciences
of Emory University in partial fulfillment
of the requirements of the degree of
Bachelor of Science with Honors

Department of Chemistry

2021

Abstract

Powering Polyvalent DNA Motors Using Exonuclease III

By Wenxiao Deng

Biological motor proteins have evolved the ability to efficiently convert the chemical energy stored in nucleotide triphosphates into mechanical work that powers locomotion and many other activities of living systems. Inspired by these biological motors, chemists and engineers have worked toward designing and assembling synthetic nano-scale machines that can convert chemical energy into controlled mechanical motion. Due to their predictability, DNA and RNA are more widely used in designing nanomotors compared to small molecules and other polymer materials. The motion of the vast majority of DNA-based motors is described by a burnt-bridge Brownian ratchet mechanism which is powered by the specific activity of enzymes. Nonetheless, DNA-based walkers fall short because of their limited speed, low endurance, and the lack of preferred directionality which is ultimately due to the lack of coordination between individual DNA legs. Standing out among the various DNA walkers is the DNA-based rolling motor that rolls on an RNA monolayer powered by RNase H. This class of DNA motor travels at an unprecedented speed with high processivity. However, the inherited instability of the RNA tracks limits this system from being applied in analytical sensing and in live cells. Therefore, it is highly desirable to design a DNA-based rolling motor that translocate on a DNA track via the rolling mechanism. In this thesis, we investigate an Exonuclease III-powered DNA motor that can roll on a DNA-based track without employing RNA fuel. We studied the specificity of Exonuclease III activity using DNA gold nanoparticle conjugates and fluorescence measurements in different enzyme conditions. Our investigations led to the design of

motors that translocate 20 μm within 30-minute durations with a sub-population of motors exhibiting superdiffusive motion. The work points toward new synthetic motor systems that are more robust and that may one day allow for real-world applications of synthetic machines.

Powering Polyvalent DNA Motors Using Exonuclease III

By

Wenxiao Deng

Khalid Salaita, Ph.D.

Adviser

A thesis submitted to the Faculty of Emory College of Arts and Sciences
of Emory University in partial fulfillment
of the requirements of the degree of
Bachelor of Science with Honors

Department of Chemistry

2021

Acknowledgements

This project would not have been accomplished without the tremendous support and encouragement of my advisor Dr. Khalid Salaita. I am extremely grateful to have Dr. Salaita as my research advisor and I appreciate the feedback and guidance he provided throughout this process. I am also thankful for the opportunity to join his lab, which further inspired my interest in basic science research and motivated me to continue my study in graduate school.

I would like to express my heartfelt gratitude to Dr. Alisina Bazrafshan for his mentorship. Dr. Bazrafshan has dedicated tremendous amount of time on my growth as a researcher from a neophyte. He has mentored me on different aspects of chemical research including experimental design, data analysis, and professional skills such as presenting. I sincerely appreciate his kindness and patience on mentoring me and for going above and beyond his role. I feel fortunate to learn under his directions.

I am also thankful to my committee members Dr. Vincent Conticello and Dr. Le Chen for their encouragement and support during my time at Emory. I enjoyed the lectures on biomolecular chemistry by Dr. Conticello and the lectures on statistics by Dr. Chen, from which I learned a lot. I am grateful that you agreed to be part of my committee.

Lastly, I would like to thank all the members of the Salaita lab for maintaining a welcoming and inclusive research atmosphere. A special word of gratitude is due to Yuesong Hu who critiqued and commented on several parts of this thesis.

Table of Contents

1. Introduction	1
1.1 Background.....	1
1.2 Aim and Scope.....	7
2. Experimental Methods.....	12
2.1 Preparation of gold surface	13
2.1.1 Thermal evaporation of gold films.....	13
2.1.2 Preparation of imaging chambers	13
2.1.3 Fabrication of DNA monolayers on Au surface	13
2.2 Fabrication of DNA monolayer on glass surface	14
2.3 Synthesis of DNA-functionalized silica beads	16
2.3.1 Synthesize of azide-functionalized particles	16
2.3.2 Functionalization of DNA-coated silica particles	16
2.4 Preparation of Rolling solution and imaging.....	17
2.5 Trajectory Analysis.....	17
2.6 Synthesis and characterization of DNA-functionalized Gold Nanoparticle	18
2.6.1 Synthesis of DNA-functionalized particles.....	18
2.6.2 Determining Gold Nanoparticle Loading Density	18
2.6.3 Preparation of Gold Nanoparticle Solution & Plate reader Reading.....	19
3. Results	19

3.1 Gel electrophoresis	24
3.2 Assembling DNA fuels on gold surface	26
3.3 Assembling DNA fuels on glass surface	28
3.4 Fluorescence-based kinetic assay for Exonuclease III activity.....	34
3.4.1 Quantification of DNA loading density and quenching efficiency	35
3.4.2 Specificity and reactivity of Exo III	38
4. Conclusions.....	43
5. References.....	46

List of Figures

Figure 1.....	2
Figure 2.....	3
Figure 3.....	5
Figure 4.....	6
Figure 5.....	7
<i>Figure 6.....</i>	<i>9</i>
Figure 7.....	10
Figure 8.....	11
Figure 9.....	15
Figure 10.....	20
Figure 11.....	23
Figure 12.....	23
Figure 13.....	26
Figure 14.....	27
Figure 15.....	28
Figure 16.....	29
Figure 17.....	30
Figure 18.....	31
Figure 19.....	33
Figure 20.....	34
Figure 21.....	35
Figure 22.....	36

Figure 23.....	37
Figure 24.....	38
Figure 25.....	40
Figure 26.....	41
Figure 27.....	42
Figure 28.....	42
Figure 29.....	45

List of Tables

Table 1 21

Table 2 22

1. Introduction

1.1 Background

Biological motors are involved in numerous operations in living systems, performing complex tasks efficiently due to their in-situ energy conversion capability for mechanical movement. Biological motor proteins such as myosin, kinesin, and dynein are responsible for a variety of critical processes in life such as cargo transport and cell division.¹ As shown in **Figure 1**, Kinesin can travel along the microtubules for several micrometers within seconds through ATP hydrolysis.² The fascinating potential application for these nanomachines has been long envisioned. Accordingly, it is of great interest to design synthetic nano and micromachines to develop next-generation sensors, molecular computers, and drug delivery platforms.³

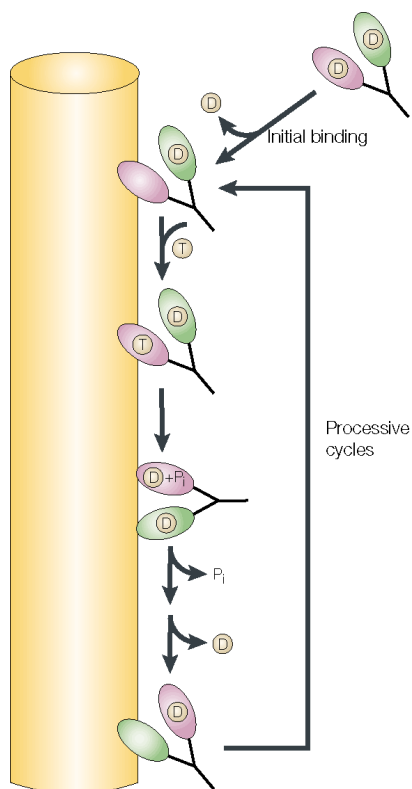


Figure 1. Kinesin moves along microtubules by taking many steps from one dimer to the next without falling off in a processive way. Throughout the catalytic cycle, one of the head is kept in the tight-microtubule-bound form (with ATP) and the other one is in an ADP-bound form. (Figure is adopted from Woehlke et al.² with permission.)

Synthetic motors work by different principles to convert energy sources of choice to mechanical energy. Ren et al. designed a bimetallic micromotor powered by a synergistic of catalytic reactions of chemical fuels and ultrasound.⁴ Zhou et al. reported a visible light-driven gold/iron oxide nanomotors in diluted hydrogen peroxide solutions.⁵ Among all the nanomotor designs, DNA has been used to construct a variety of nanomotors since DNA molecules offer several key advantages that enable rational design, experimentation, and elucidation of key parameters in nanoscale motor performance. These key advantages include the ability to tailor 3D structure with molecular precision, ease of synthesis and functionalization in addition to the tunability of DNA hybridization and hydrolysis reaction kinetics. Therefore, DNA-based machines offer the most promise in recapitulating the properties of natural motor proteins.

DNA motors translocate by converting chemical energy into mechanical motion using a mechanism called the “burnt-bridge Brownian ratchet”.⁶ This mechanism involves binding between DNA “legs” and complementary oligonucleotide “footholds”, followed by a transformation step that diminishes the affinity of the DNA leg to the occupied foothold. This transformation biases the motion to an adjacent unoccupied foothold site and moves the motor away from previously visited sites.⁷

Early examples of BBR motors have 1 or 2 DNA “legs”.^{8,9} These motors are programmed to walk along defined tracks and therefore are named “DNA walkers”. These DNA walkers can take a limited number of steps. This limitation is due to the spontaneous dissociation

of DNA walkers from their tracks.¹⁰ Introduction of additional number of legs increases the affinity of the motors for their tracks and therefore decreases the probability of dissociation. Ellington and coworkers increased the number of steps taken by a monoleg DNA walker up to 38 steps by increasing the number of legs.^{11, 12} However, increasing the number of legs leads to an increase in the number of steps a motor can take before dissociation (processivity) at a cost of diminished velocity.¹³ Cha et al. designed a polyvalent DNAzyme motor capable of moving along the nanotube track for 3 μm in 30 hours with a translocation speed of 1nm min^{-1} (**Figure 2**).¹⁴ This study shows that unidirectional and processive movement of this motor can be achieved by increasing the number of legs on the motor at the sacrifice of motor speed. This points to a trade-off between polyvalency and speed in DNA walkers.

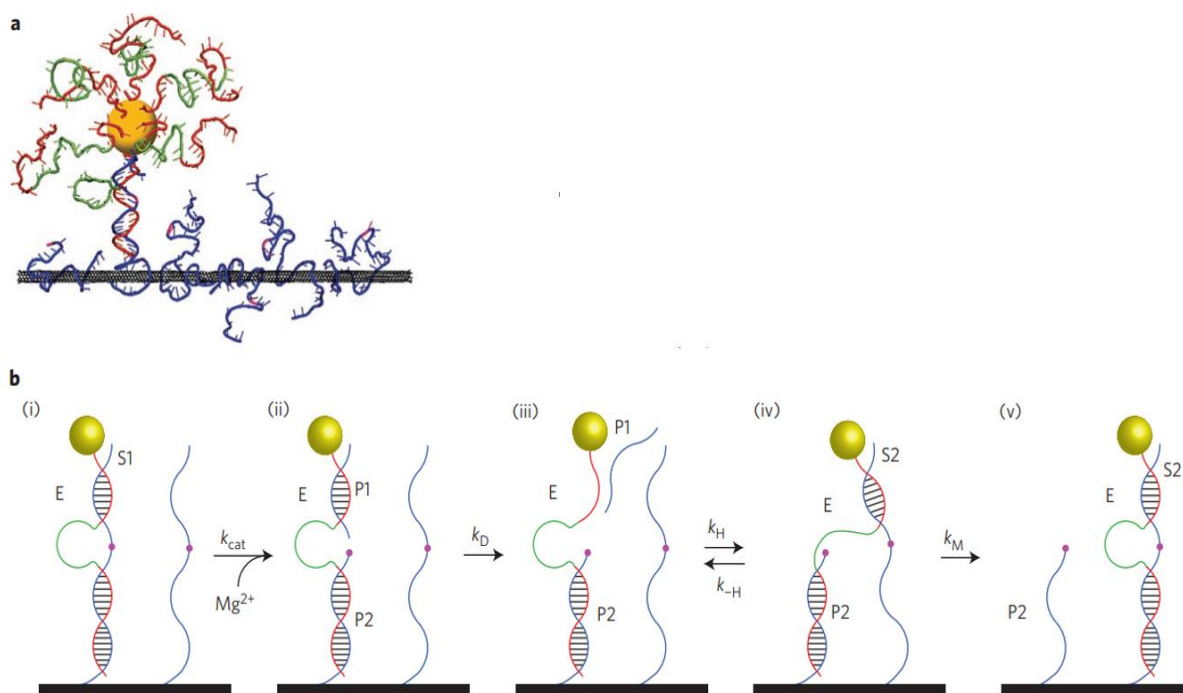


Figure 2. The DNAzyme-based molecular motor that moves along a carbon-nanotube track. a) Molecular model of a 10-23 DNAzyme-based motor on an RNA-

coated nanotube track. Approximately 20 10-23 DNAzyme strands are attached to the CdS nanocrystal (shown in yellow) with the two recognition arms (shown in red) and the catalytic core (shown in green). The CdS nanocrystal is used for the cargo and the carbon-nanotube (shown in black) coated with RNA strands (shown in blue) is used as the track. b) Walking principle of the DNAzyme-based motor. The DNAzyme-based motor moves along the nanotube track by converting the chemical energy of RNA into mechanical motion. Initially, the motor binds to the RNA coated on the nanotube and cleaves the RNA at the point marked with pink in the presence of Mg^{2+} , producing two fragments of RNA (P1 and P2). After P1 dissociates from the motor leg, the unbound recognition arm binds to the complementary region on an adjacent RNA. The rest of the DNAzyme strand leaves P2 and moves to the RNA strand that the other part of it hybridizes to. (Figure is adopted from Cha et al.¹⁴ with permission.)

An exception to this trade-off is a DNA micromotor that rolls on a surface modified with complementary RNA strands powered by RNase H.⁶ The motor system is comprised of DNA-coated 5 μm silica beads that hybridize to a surface coated with complementary RNA strands. RNase H selectively hydrolyses the RNA duplexed to DNA, leaving the DNA strands on the motor intact as the structural elements within the assemblies after hydrolysis so that the DNA legs can move by binding new single-strand RNA. The driving force of this movement is derived from the free energy of hybridization between the DNA legs on the motor and the fuel strands on the surface as shown in **Figure 3**. This system is reported to be the fastest and most processive DNA-based motor to date and can achieve translocation in mm distances with velocities up to 5 $\mu\text{m}/\text{min}$. The merit of these motors is attributed to their ability to roll instead of walking, which overcomes the fundamental trade-off between processivity and speed when increasing polyvalency.

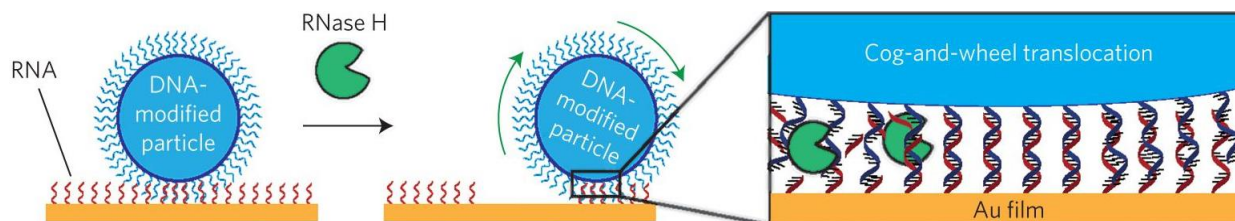


Figure 3. The schematic of burnt-bridge Brownian mechanism powered by RNase H. Particles coated with DNA strands are immobile on a surface with complementary RNA strands until RNase H is added. (Figure is adopted from Yehl et al.⁶ with permission.)

This rolling mechanism is not unique to particles with microscale size. It has also been employed to power the motion of nanoscale origami structures and DNA gold nanoparticle conjugates. By displaying DNA legs on a DNA origami scaffold, Bazrafshan et al. tuned design parameters such as polyvalency, DNA leg distribution, DNA leg density as well as chassis flexibility. In addition, motor net displacement and diffusion pattern for each case were measured (**Figure 4**).⁷ This study shows that a rigid anisotropic chassis coupled with a high density of DNA legs present on all sides of the body results in nanoscale motors that can translocate micrometer distances with instantaneous velocities of up to 100 nm/min. Importantly, designing motors that cannot roll (display of same density of DNA “legs” only on one side of the motor) results in diminished net displacements and diffusive motion. The high density of DNA legs on the particle prevents it from dissociating from the track and offers the key ability to roll instead of walk across the surface. Therefore, translocating via rolling is instrumental to impressive speeds and net displacement of the DNA origami-based motor when employed in the Burnt-bridge Brownian mechanism powered by RNase H. The comparison between the rolling mechanism and the walking mechanism is shown in **Figure 5**.

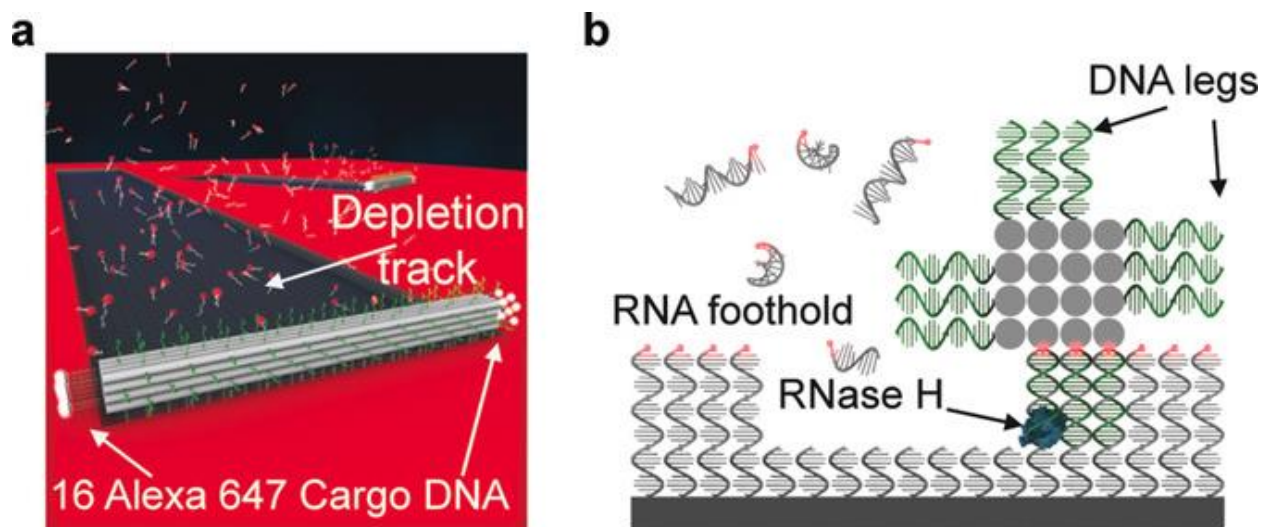


Figure 4. Design of DNA origami motor consisting of a bundle of 16 DNA double helices. a) Illustration of DNA origami motor motion. The origami is coated with DNA that is complementary to the surface RNA. Upon the addition of RNase H, hybridization between motor and the surface is cleaved. This reaction releases the fluorophores coated on the surface and leads the motor to move through a cog-and-wheel mechanism, which allows the origami motor to roll on the surface. A depletion track underneath the motor is observed due to the depletion of fluorophores on the surface. b) Schematic of DNA origami motor powered by RNase H. RNase H selectively cleaves RNA in the DNA-RNA chimera, therefore driving the motion from the free energy of binding new ssRNA and biasing the motion away from consumed fuel. (Figure is adopted from Bazrafshan et al.⁷ with permission.)

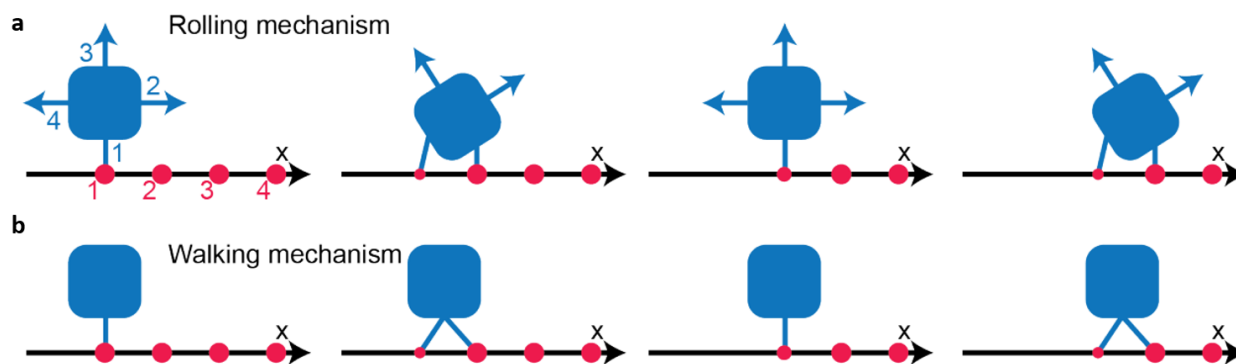


Figure 5. Illustration for a DNA origami motor travels via a) rolling mechanism and b) walking mechanism. The footholds are labelled in red, and the DNA legs on the origami motors are labelled in blue. (Figure is adopted from Bazrafshan et al.⁷ with permission.)

1.2 Aim and Scope

Despite the high speed and processivity of these above-mentioned rolling motors, these motors currently rely on RNA molecules for fuel. RNA is inherently unstable due to the hydroxyl group on the C2' of the ribose sugar, which makes it susceptible to auto-cleavage and limits the bench-life of the RNA surfaces to a week. Furthermore, these motor systems cannot be interfaced with living cells as they secrete many RNases. For these DNA systems to be applicable as point of care sensors or interfacing biological cells, design of reactions that power DNA based rolling motors with DNA fuel is desirable. The average half-life for DNAs is over a hundred years,¹⁵ and DNA can be presented to living cells. Hence, it is expected if a DNA based motor uses DNA as fuel, the microfluidic chips can last for weeks and motors can be presented to interact with living cells.

To design a DNA fuel for DNA motors, DNA fuels need to be hydrolyzed specifically when bound to DNA legs. As elaborated before, Yehl et al. applied RNase to selectively

hydrolyze RNA duplexed to DNA to power the microparticle motor. Inspired by this, we chose Exonuclease III as a candidate to specifically hydrolyze the DNA-DNA duplex in the DNA based motor system. Exonuclease III is derived from *Escherichia coli* and catalyzes the stepwise removal of nucleotides from the 3' blunt ends of DNA duplexes¹⁶, leaving the other strand intact (**Figure 6b**). It is reported to have some structural and functional similarities with RNase H.¹⁷ The similarities in structures between RNase H and Exonuclease III suggest that RNase H adopts a hydrolytic, single divalent metal ion mechanism that is similar to the Asp-His-H₂O mechanism proposed for Exonuclease III as shown in **Figure 6c**, whereas their different substrate binding and catalytic specificity are attributed to the difference in their surrounding loop regions.

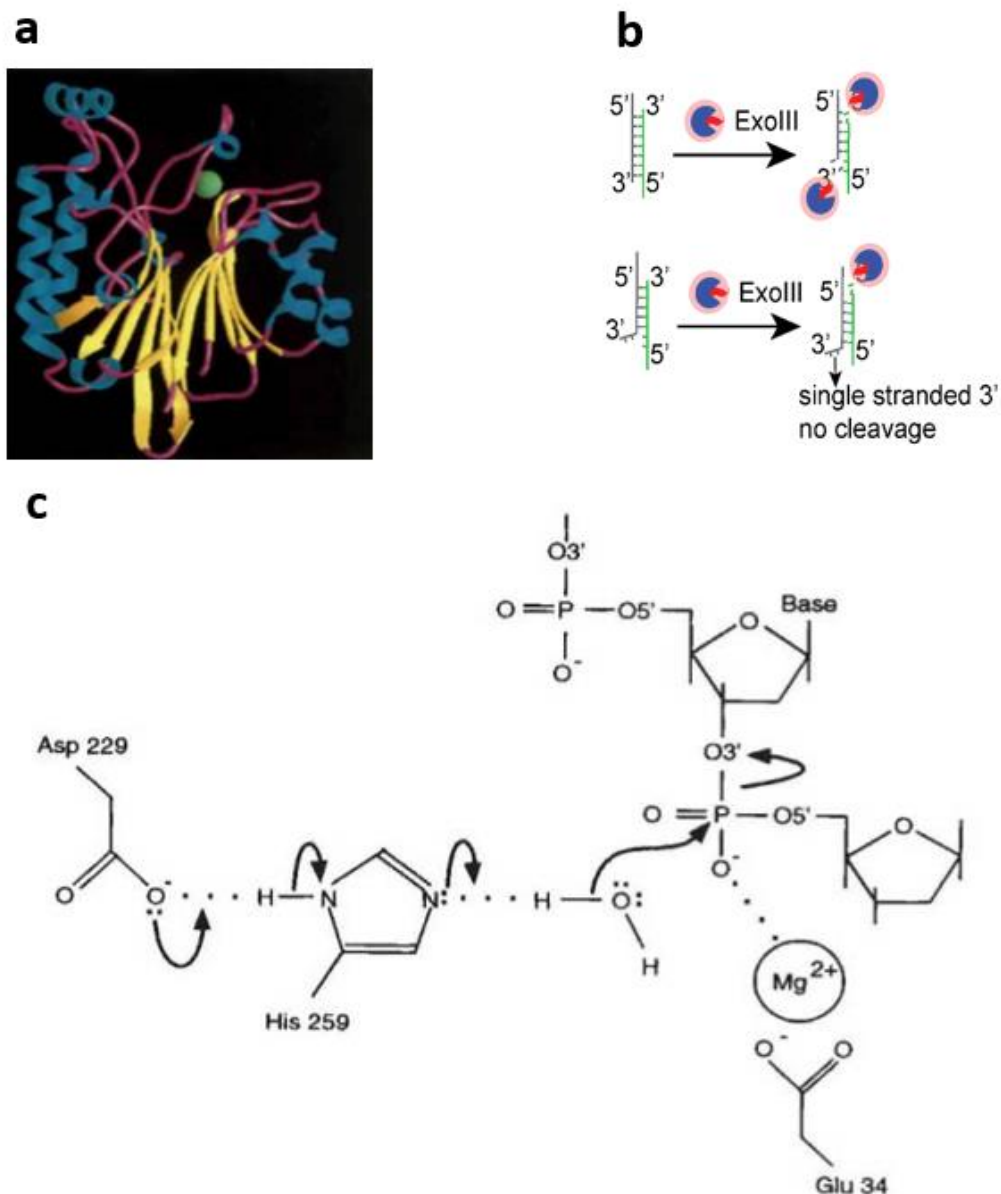


Figure 6. Structure and Activities of Exonuclease III. a) 1.7Å resolution structure of Exonuclease III¹⁷. This enzyme is a compact, globular protein of rough dimensions 55Å×50Å×45Å. It consists of two β -sheets and four α -helices on their sides. b) Exonuclease III recognizes 3' blunt end of DNA duplexes and cleaves phosphodiester bonds successively. c) the Asp-His-H₂O reaction mechanism proposed for the hydrolytic cleavage of the phosphorus-oxygen bond by Exonuclease III. This mechanism may also apply to RNase H for its putative catalytic residues: Asp 70 and His 124, versus Asp 229

and His 259 in Exonuclease III. (Figure 6a and 6c are adopted from Mol et al.¹⁷ with permission.)

Luo et al. reported the selectivity of Exonuclease III towards the blunt 3' end of DNA duplex using denaturing polyacrylamide gel electrophoresis (PAGE).¹⁸ Notably, Exonuclease III only digests the strands with the blunt 3' end without cleaving the other strands in the system (**Figure 7**).

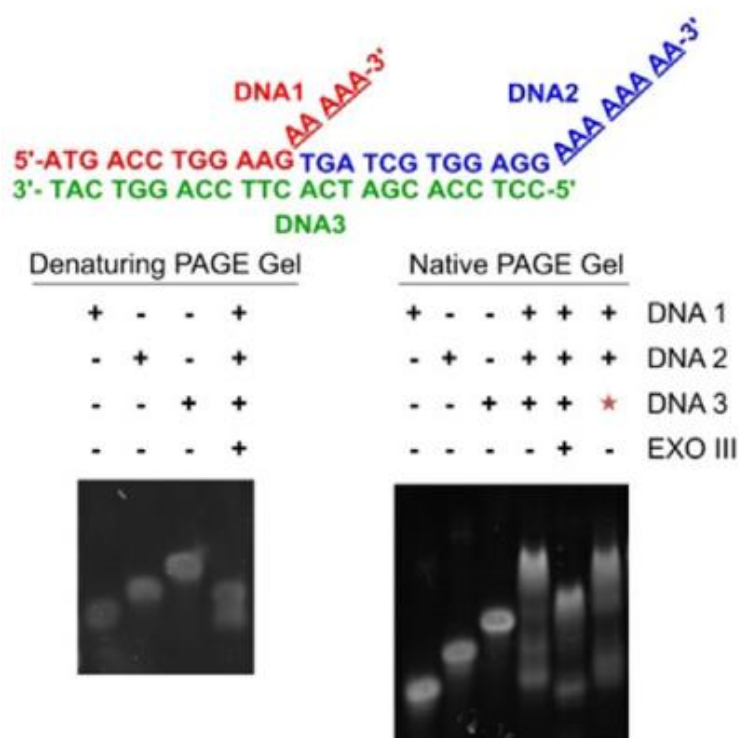


Figure 7. Gel electrophoretic analysis of Exonuclease III activity. DNA 3 is hybridized together with another two DNA strands, and a blunt 3' end is created on the 3' end of DNA 3. In Denaturing PAGE Gel, when Exonuclease III was added, only the band representing DNA3 disappeared while the bands for the other two DNA strands remained intact, indicating that Exonuclease III only digests DNA 3. In the Native PAGE Gel, when DNA 3 was added to the digested solution, the band representing double-stranded DNA was regenerated. The remaining bands were attributed to the complex of DNA 2 and the residues of DNA 3. (Figure is adopted from Luo et al.¹⁸ with permission.)

Qu et al. developed an Exonuclease III-powered DNA walker that moved on DNA tracks on a gold nanoparticle surface via a “burnt-bridge Brownian ratchet” mechanism (**Figure 8**).¹⁹ The DNA walker is first hybridized to the SNA surface, creating a blunt 3' end for Exonuclease III cleavage. When added to solution, Exonuclease III recognizes the blunt 3' end and stepwisely removes mononucleotides from it, gradually releasing the DNA walker. The released walker then hybridizes to another DNA strand on the nanoparticle and triggers a new cleavage process. The processivity of DNA walkers is also claimed to be guaranteed due to the high hydrolysis rate of Exonuclease III walkers, which is 100-1000 folds greater than that of DNAzymes and endonucleases.^{19, 20}

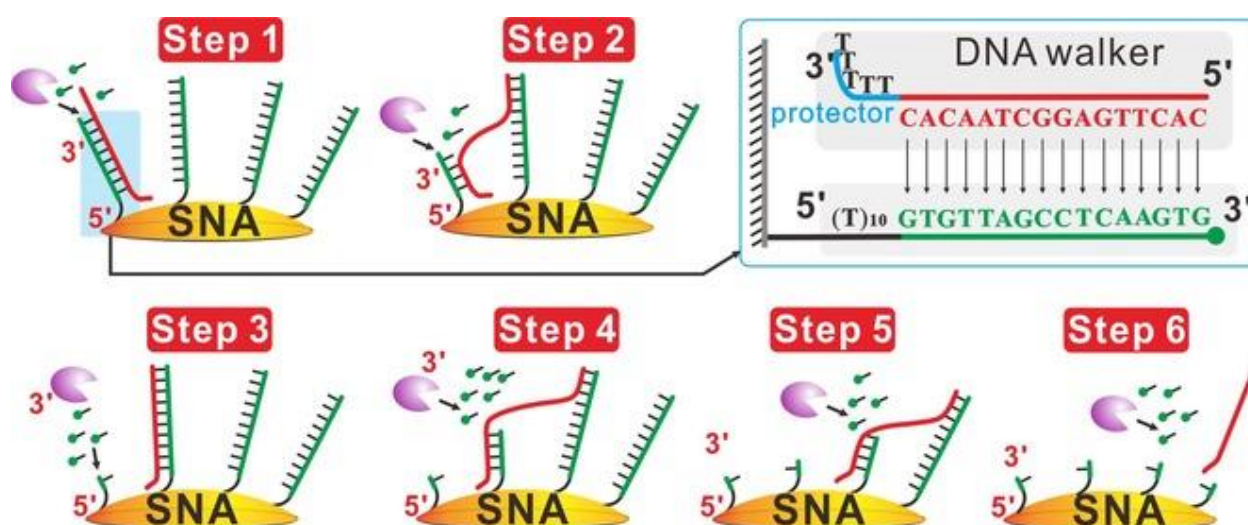


Figure 8. Schematics for Exonuclease III-based DNA walker that moves on a DNA-functionalized gold nanoparticle. The walker is labeled in red and moves on the SNA surface through Exonuclease III selectivity. (Figure is adapted from Qu et al.¹⁹ with permission.)

The Exonuclease III based walker is monopedal, which is highly susceptible to dissociation. The walking mechanism it adopts also constrains the potential to increase

motor polyvalency for enhanced processivity for the drop in motor speed associated. Given the verified specificity and fast hydrolysis rate of Exonuclease III, we hypothesize that the kinetics of Exonuclease III can be optimized to design a DNA counterpart of RNA-based rolling motor designed by Yehl et al. By expanding the fuel diversity of polyvalent DNA motors, the limitations associated with RNA tracks can be addressed and hence enable DNA based rolling motors to real world applications.

2. Experimental Methods

All chemicals were purchased from Sigma-Aldrich unless otherwise noted. Stock solutions were made using Nanopure water (Barnstead Nanopure system, resistivity = 18.2 M Ω), herein referred to as DI water. All oligonucleotides were custom synthesized by Integrated DNA Technologies (Coralville, IA), stored at -20°C, and used without purification. Their sequences together with the functional group modifications are summarized in Table 1. Thin Au films were generated by using a home-built thermal evaporator system. Motor translocation on gold surfaces were performed in custom-designed imaging chambers etched from ¼ inch-thick white Delrin (McMaster-Carr #8573K15). All motor translocation measurements on glass surfaces were performed in IBIDI sticky-Slide VI0.4 17 × 3.8 × 0.4 mm channels. Azido-PEG4-NHS ester was purchased from Click Chemistry Tools (Scottsdale, AZ, USA, product# AZ103-1000). Exonuclease III was purchased from New England BioLabs (Ipswich, MA, USA, product# M0206SVIAL). All computations were performed using MATLAB 2016a or later on a conventional laptop computer or desktop computer in lab. The experimental methods were adapted from the work from Yehl et al., Bazrafshan et al., and Blanchard et al. ^{6, 7,}

2.1 Preparation of gold surface

2.1.1 Thermal evaporation of gold films

A glass slide of size 25 × 75 mm was sonicated in DI water for five minutes. The glass slide was sonicated again in fresh DI water for five minutes. Next, the glass slide was sonicated in propanol for five minutes and was then dried under a stream of N₂. The slide was placed into a home-built thermal evaporator chamber located at the Physics Department of Emory University. The pressure of the chamber was first reduced to 50×10^{-3} Torr. Then the pressure of the chamber was reduced to $1-2 \times 10^{-7}$ Torr by purging the chamber with N₂ for three times using a turbo pump with a liquid N₂ trap. Chromium was deposited onto the slide at the rate of 0.2 \AA s^{-1} . Next, 4nm of gold was deposited at a rate of 0.4 \AA s^{-1} .

2.1.2 Preparation of imaging chambers

Imaging chambers were made from ¼ inch-thick white Delrin using a 60-watt CO₂ laser cutter (Universal Laser Systems, model VLS 4.60). The chambers are of size 25 × 75 mm with 8 elliptical holes. One side of the Delrin was layered with not reactive, double-sided sticky type (McMaster-Carr #7602A53). After being rinsed in acetone and dried using kimwipe and nitrogen stream, imaging chambers were taped to the Au-coated glass slides.

2.1.3 Fabrication of DNA monolayers on Au surface

Each well was washed with DI water for three times. Next, 40µl of 1µM disulfide-modified DNA anchor was incubated with the surface for 12 hours under 1M KHPO₄. The chambers were sealed with parafilm to prevent evaporation. The wells were then washed with DI water for three times. Next, the surface was incubated with 100 µl of 100 µM SH(CH₂)₁₁(OCH₂CH₂)₆OCH₃ (SH-PEG) solution in ethanol for 6 hours followed by thrice

ethanol wash and thrice water wash. At last, the DNA fuel was hybridized to the surface through the addition of 100 μ l of 100 μ M complementary DNA in 1x Exonuclease III buffer (66mM Tris-HCl 660 μ M MgCl₂, PH=7.5) for 12 hours.

2.2 Fabrication of DNA monolayer on glass surface

A glass slide of size 25 mm \times 75 mm was sonicated in DI water for 15 minutes. The sample was then sonicated in ethanol for 15 minutes. The slide was rinsed by DI water for six times and was then dried by a stream of N₂. The slide was then soaked in piranha solution (v/v=3:7 hydrogen peroxide/sulfuric acid) for 30 minutes. The slide was then rinsed with DI water in a 200mL beaker for 6 times and washed with ethanol for three times. The slide was then incubated in a 200mL beaker containing 2% (v/v) APETES in ethanol for 1 hour, and then rinsed with ethanol for 3 times and baked in an oven (~110°C) for 30 minutes. IBIDI channel was then attached to the glass slide. Each well was then incubated in ~50 μ l of 10 mg/mL of NHS-PEG₄-azide (Click Chemistry Tools) in 0.1 M NaHCO₃ (pH=9) for 1 hour. The channels were then washed by DI water for three times and the remaining water in the channels was removed by pipetting. Each channel was then incubated with click solution (10 μ M alkyne modified DNA (anchor strand), 50 μ M THPTA, 10 μ M CuSO₄ and 1 mM sodium ascorbate in 1 M potassium phosphate buffer) for one hour. The channels were rinsed with 5 mL of DI water. Lastly, each channel was incubated with 100 μ l of 100 μ M complementary DNA fuel in 1x Exonuclease III buffer (66mM Tris-HCl 660 μ M MgCl₂, PH=7.5) for 12 hours at room temperature. The wells were preserved by sealing with parafilm for each step to prevent evaporation. A schematic of Cy3-RNA monolayer synthesis and characterization was shown in **Figure 9**.

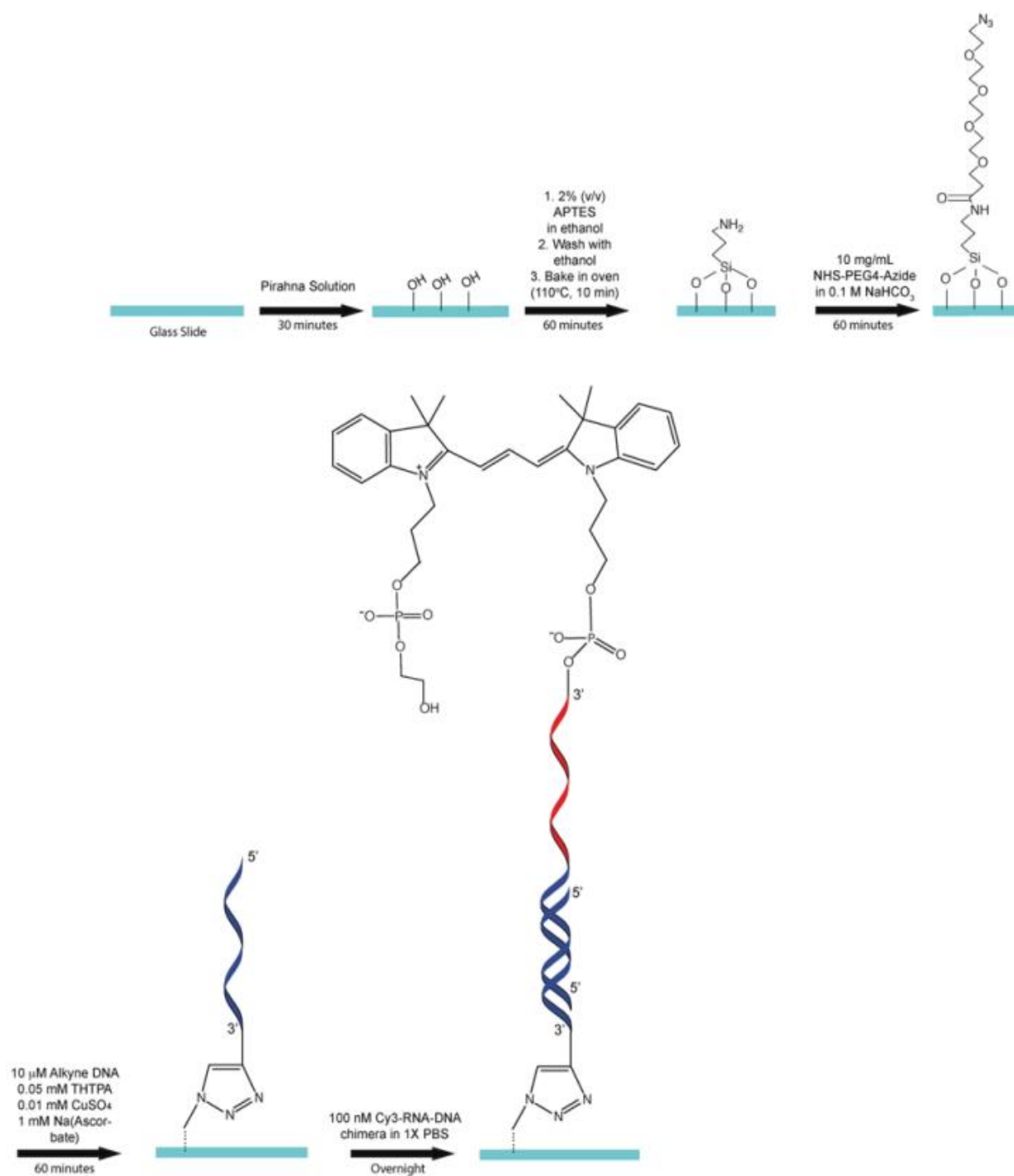


Figure 9. Schematic of the surface preparation steps for RNA monolayer on glass surface. (Figure is adopted from Bazrafshan et al.⁷ with permission.)

2.3 Synthesis of DNA-functionalized silica beads

2.3.1 Synthesis of azide-functionalized particles

A mixture of 1 mg of 5 μm animated silica beads (Bangs Laboratory) and 1 mg of *N*-hydroxysuccinimidyl azide heterobifunctional linker was diluted in 100 μL of dimethylsulfoxide (DMSO) and 1 μL of a 10 \times diluted triethylamine stock solution in DMSO and incubated overnight for 24 hours. Next, 1 mL of DI water was added to the azide-modified particles and the sample was centrifuged at 15000 revolutions per minute (r.p.m) for 5 minutes. The supernatant was removed by pipetting and the remaining particles centrifuged down at the bottom of the Eppendorf were resuspended in 1mL of DI water. This process was repeated for 7 times, and in the last step, the particles were resuspended in 100 μL of DI water. The particles were stored at 4°C in the dark.

2.3.2 Functionalization of DNA-coated silica particles

5 μL of 1 mM alkyne modified DNA was added to 5 μL of the azide-functionalized particles. This mixture was diluted with 25 μL of DMSO and 5 μL of 2M triethyl ammonium acetate buffer (pH 7.0). 4 μL of 5 mM ascorbic acid was added to the reaction. 2 μL of 10 mM Cu-TBTA (tris((1-benzyl-1*H*-1,2,3-triazol-4-yl)methyl)amine) stock solution in 55 vol% DMSO was added to the mixture and incubated for 24 hours.²² The resulting DNA-functionalized particles were purified by five-minute centrifugation at 15000 r.p.m. The supernatant was removed by pipetting and the particles were resuspended in 1x PBS supplemented with 10% Triton-X solution. This process was repeated for 7 times, and the particles are resuspended in 1x PBS only in the fourth to sixth washes. In the last wash, the particles were resuspended in 50 μL of 1x PBS. The particles were stored at 4°C in the dark.

2.4 Preparation of Rolling solution and imaging

10 μL of 10x Exonuclease III buffer (660mM Tris-HCl, 6.6mM MgCl_2 , pH=8.0), 10 μL of formamide, 10 μL of 7.5% triton X solution, 1 μL of 1mM DTT, and 1 μL of Exonuclease III enzyme and 68 μL of DI water were mixed to make the rolling solution (1x Exonuclease III buffer, 10 μM DTT, 10% v/v formamide and 0.75% v/v triton X) with varying concentrations of Exonuclease III enzyme concentration.

Prior to use, the channel was gently rinsed with 3mL 1x PBS and placed on the STORM microscope. The fluorescence intensity of the surface was first checked under epi fluorescence microscope FITC channel at 100x magnification. 10 pM of particles were added to the channel and were given around 2 minutes to bind to the surface. The channel was then gently washed with 1 mL 1x Exonuclease III buffer to remove any unbounded particles. The rolling solution was then added to the surface to initiate the reaction.

Then, 5 regions of interests (ROIs) were selected using the bright field channel on the STORM microscope at 100x magnification. Particle motion was measured using time-lapsed imaging of RICM channel for around 15 minutes at a 30-second time interval. After the time lapse finished, pictures of depletion tracks on the surface were taken to confirm that the motion captured in the videos were due to Exonuclease III hydrolysis instead of diffusion.

2.5 Trajectory Analysis

Image analysis was performed using Fiji (Image J) and MATLAB 2019b (Math Works). Data from particle tracking was obtained using MOSAIC Image J plugin in the form of a data table transferred to MATLAB using a custom script for the analysis of motion.²³

The mean square displacement of each trajectory was calculated from custom-written MATLAB codes and was then plotted against lag time. Alpha value (the anomalous diffusion exponent α) was reported as the slope of log-log fit to the MSD vs lag time plot for each trajectory.

2.6 Synthesis and characterization of DNA-functionalized Gold Nanoparticle

2.6.1 Synthesis of DNA-functionalized particles

600 μL of 15 nm gold nanoparticles were mixed with 15 μL of 100 μM DNA fuel and 7.5 μL of 100 μM thiolated DNA anchor in a glass vial. The sample was frozen in the freezer and thawed in room temperature. This process was repeated for three times. The solution was transferred to an Eppendorf and 478 μL of 1x PBS was added to the Eppendorf. The particles were purified by centrifugation for 20 minutes at 15000 r.p.m. The supernatant was removed by pipetting out 1mL of solution, and the remaining particles were resuspended in 1mL of 1x PBS solution. This process was repeated for 3 times. In the last wash, the particles were resuspended in 100 μL of 1x PBS buffer. To hybridize guide DNA to the gold nanoparticle, 100 nM short guide DNA was incubated with the particles overnight on the orbital shaker at room temperature. On the next day, the particles were washed with PBS once and stored at 4°C in the dark.

2.6.2 Determining Gold Nanoparticle Loading Density

After gold nanoparticles were functionalized with DNA, their concentration was determined by UV-VIS at maximum absorbance of 520 nm (extinction coefficient = $3.67 \times 10^8 \text{ M}^{-1} \text{ cm}^{-1}$). To make the calibration curve, samples containing 0, 0.1, 1, 10, 100, 1000 nM of free FAM tagged DNA fuel and 0.5 nM of 15 nm gold nanoparticles coated with

poly-T were prepared. Fluorescence intensity of each well was then measured (485/528 nm excitation/emission) using a Bio-Tek Synergy HT plate reader.

DNA fuel coated nanoparticles were prepared by mixing 0, 0.005, 0.025, 0.05, 0.25, 0.5 nmol of FAM tagged DNA fuel with 100 μ L of 15 nm gold nanoparticles functionalized with 0.25 nmol of thiolated-DNA anchor strands. After the fluorescence intensities of 0.5 nM of each gold nanoparticle sample were measured for using plate reader, 1 μ L of 1 mM Dithiothreitol (DTT) was added to each well and the fluorescence intensities were measured again. The concentration of DNA fuel released from the particles was quantified. The loading density of 15 nm gold nanoparticles was calculated by dividing the concentration of released DNA fuel by the concentration of gold nanoparticles.

2.6.3 Preparation of Gold Nanoparticle Solution & Plate reader Reading

100 μ L of gold nanoparticle reaction solution (10 μ M Dithiothreitol (DTT), 0.5 nM 15 nm gold nanoparticles, 1x Exonuclease III buffer) was added to each well. A 1-hour kinetics measurements of fluorescence intensity with 1-minute time interval was then performed right after Exonuclease III addition.

3. Results

The proposed design for an Exonuclease III-powered DNA motor is shown in **Figure 10**. The strands are engineered in a way that only when DNA leg binds to fuel substrates on the surface, a 3' blunt end of a duplex is formed (**Figure 11**). The oligonucleotide sequences designed by Yehl et al. have a blunt 3' end on their fuel strand when the particle is bound to the surface. Therefore, the DNA leg is tuned to present a single stranded 3' which is hypothesized to be Exonuclease III resistant and the DNA

counterparts of the RNA fuel sequences used by Yehl et al. are adopted in this study. The DNA fuel is labeled with a FAM fluorophore to enable visualization of fuel consumption. The sequences of oligonucleotides used in this study together with the structures of the DNA modifications are summarized in Table 1 and Table 2.

Hybridization of DNA legs on the particle to DNA fuel on the surface immobilizes the motors. Upon addition of Exonuclease III, DNA fuels that are duplexed to the DNA leg (particle guide DNA) are consumed. According to the NUPACK analysis, DNA legs are protected by 5 non-hybridizing nucleotides (**Figure 12**). Therefore, digestion of DNA legs is blocked, and they can continue to bind next available fuels and triggers a new cleavage process, leading to motion of the particle.

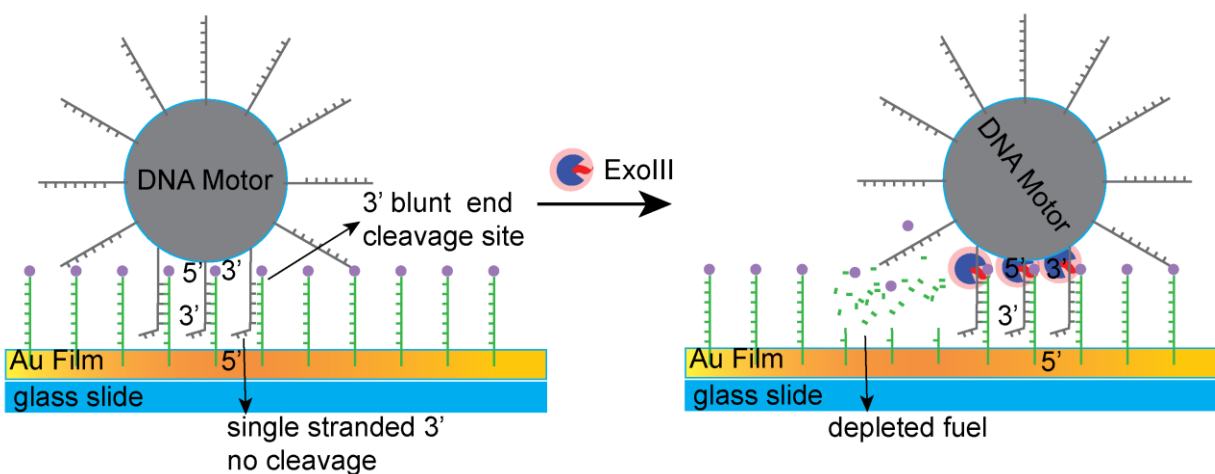


Figure 10. Schematic design for DNA rolling motors fueled by DNA on a gold surface. DNA-modified particles are hybridized to a DNA monolayer. The sequences are designed that upon addition of Exonuclease III, the DNA fuel hybridized to the particles are selectively cleaved, making it possible for the particle to roll.

Name	Sequence (5'-3')
Thiolated DNA Anchor	GAGAGAGATGGGTGCTTTTTTTTTTTTTTTT/5ThioMC6-D/
Alkyne DNA anchor	/5AmMC6/GAGAGAGATGGGTGCTTTTTTTTTTTTTTTT/35OctdU/
DNA fuel	GCACCCATCTCTCTCCCCCTCCCCATTGACT/36-FAM/
particle Guide DNA	/5Hexynyl/TTTTTTTTTTTTTTTAGTAATCAATCACAG
Short guide DNA	TTTAGTAATCAATCACAG

Table 1. The sequences of oligonucleotides and their name system in the Exonuclease III-powered DNA-fueled nanomotor design.

Modification ID	Modification name	Chemical structure
/5ThioMC6-D/	5' Thiol Modifier C6 S-S	
/5AmMC6/	5' Amino Modifier C6	

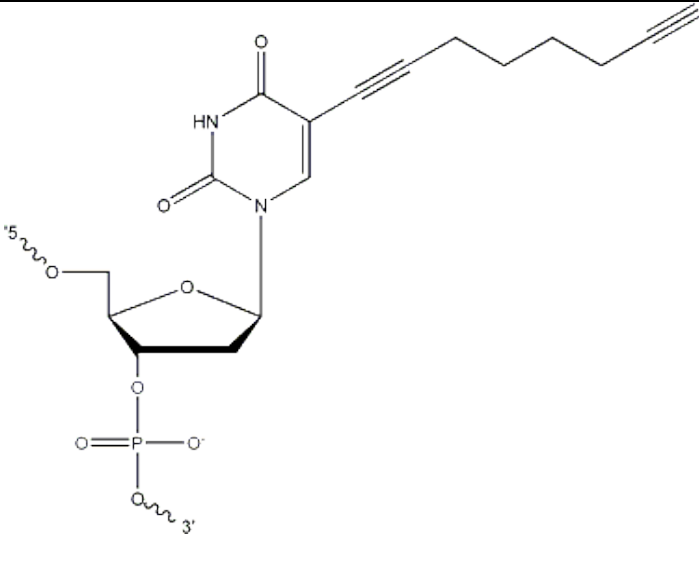
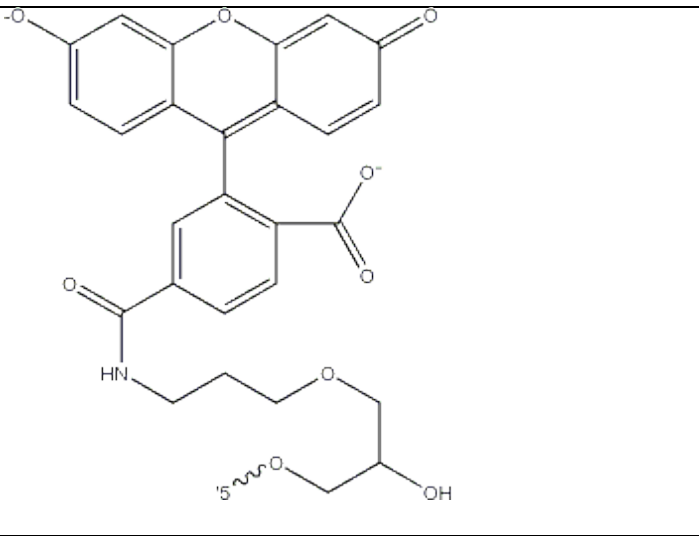
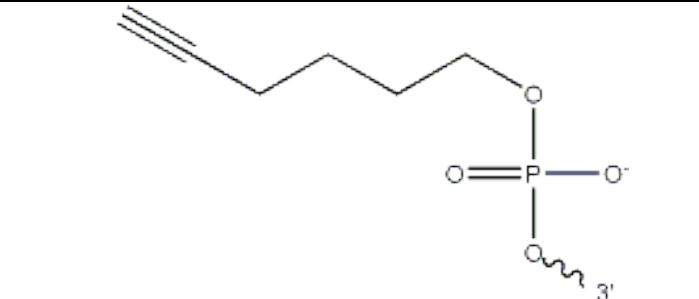
/35OctdU/	3' 5-Octadiynyl dU	
/36-FAM/	3' 6-FAM (Fluorescein)	
/5Hexynyl/	5' Hexynyl	

Table 2. Chemical structures of DNA modifications used in the Exonuclease III-powered DNA-fueled nanomotor design.

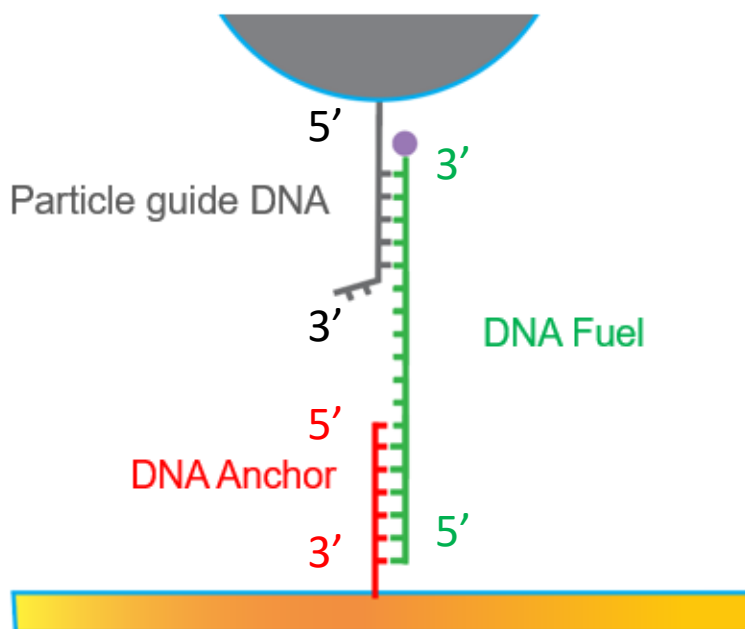
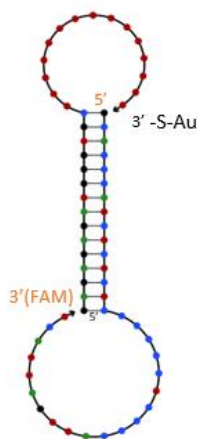


Figure 11. Illustration of hybridized oligonucleotide sequences at the particle-fuel junction. The FAM fluorophore is shown in purple and the DNA-coated particle is shown in grey.

a

MFE structure at 37.0 C

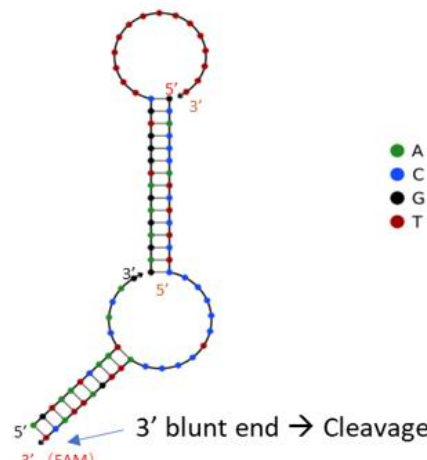


No 3' blunt end
→ No cleavage

Free energy of secondary structure: -21.52 kcal/mol

b

MFE structure at 37.0 C

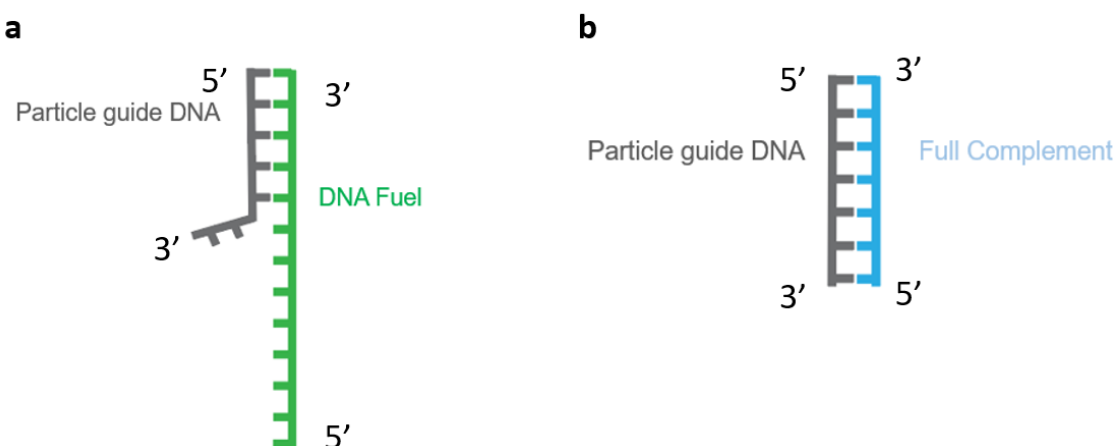


Free energy of secondary structure: -32.35 kcal/mol

Figure 12. NUPACK analysis of nucleic acid systems in the design for Exonuclease III-powered DNA motor. a) DNA anchor hybridized to DNA fuel. There is no blunt 3' end created and therefore no cleavage is expected to be initiated by Exonuclease III. b) Particle guide DNA hybridized to the duplex of DNA fuel and DNA anchor. A 3' blunt end is created such that Exonuclease III can remove nucleotides from it. The 3' end of the particle guide DNA is protected by a 5-nucleotide overhang to prevent enzyme cleavage.

3.1 Gel electrophoresis

Initially, the selectivity of Exonuclease III on the designed blunt 3' end cleavage site was tested by denaturing polyacrylamide gel electrophoresis (PAGE). **Figure 13** shows the gel electrophoretic analysis of Exonuclease III specificity. Exonuclease III only digested the DNA fuel, leaving the particle guide DNA intact (**Figure 13, well 3, 5**). However, in which the particle guide DNA was mixed with its full complement, the enzyme cleaved both the complement and the particle guide DNA as expected (**Figure 13, well 4,6**). These results represent a proof that Exonuclease III has the potential to be used as a powering-enzyme in a DNA-based rolling system.



c

	1	2	3	4	5	6
Particle guide DNA (nM)	10	-	10	10	10	10
DNA fuel (nM)	-	-	100	-	100	-
Full complement (nM)	-	100	-	100	-	100
Exo III (Units)	-	-	50	50	50	5

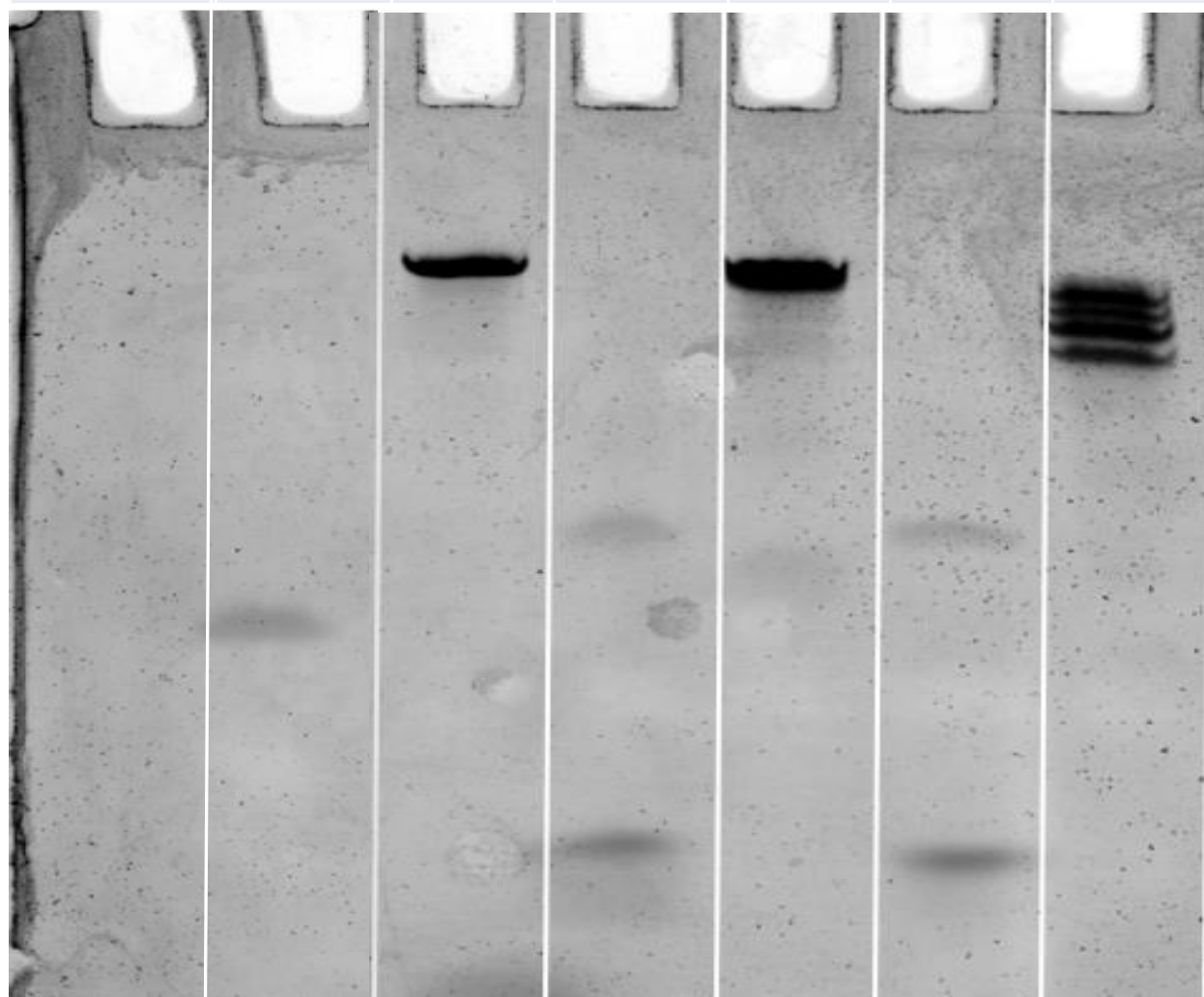


Figure 13. Gel electrophoresis analysis of fuel strand digestion by Exonuclease III.

a) *Illustration of hybridized particle guide DNA and DNA fuel. A blunt 3' end is created only on the DNA fuel. The digestion of DNA fuel only by Exonuclease III is expected.* b) *Illustration of hybridized particle guide DNA and full complement. Blunt 3' ends are created on both oligonucleotides. Digestion of both particle guide DNA and full complement by Exonuclease III is expected.* c) *Denaturing polyacrylamide gel electrophoresis (PAGE) result of Exonuclease III specificity on oligonucleotides in the designed system.*

3.2 Assembling DNA fuels on gold surface

A gold surface offers great promise to achieve a high surface intensity of DNA fuels. The maximum RNA density on a gold surface was reported to be 50,000 molecules/ μm^2 , while the maximum RNA density on a glass surface was reported to be 22,000 molecules/ μm^2 .⁶

7

DNA-functionalized 5-micron silica beads were added to a gold surface coated with complementary DNA. No motion was observed in the absence of Exonuclease III. Upon addition of 10 units of Exonuclease III, two 4 μm depletion tracks under a dimerize particle were observed after 15 minutes (**Figure 14**). In order to obtain longer depletion tracks, the reaction was performed for 30 minutes. Although motions of the particles were observed from the time-lapsed movie acquired in the bright field channel, depletion tracks on the surface were not observed in the FAM-fluorescence channel due to the low fluorescence intensity on the surface. As shown in **Figure 15**, the fluorescence intensity of the surface decreased by half after 15 minutes and approached background after 40 min. The significant loss of surface fluorescence intensity could be partly attributed to the high susceptibility of FAM to photobleaching.²⁴ In addition, the non-specific reaction between Exonuclease III and unoccupied fuels could also degrade the surface.

Furthermore, in the above experimental conditions, 10 μM of DTT was added to the surface as an enzyme stabilizing agent that is necessary to preserve the activity of Exonuclease III.²⁵ DTT is capable of effectively removing thiolated oligonucleotides from gold surfaces by replacing the thiol gold bond anchoring the DNA fuels.^{26, 27} Therefore, the conundrum of balancing the stability of surface and activity of enzyme limits the performance of DNA motors on gold surfaces.

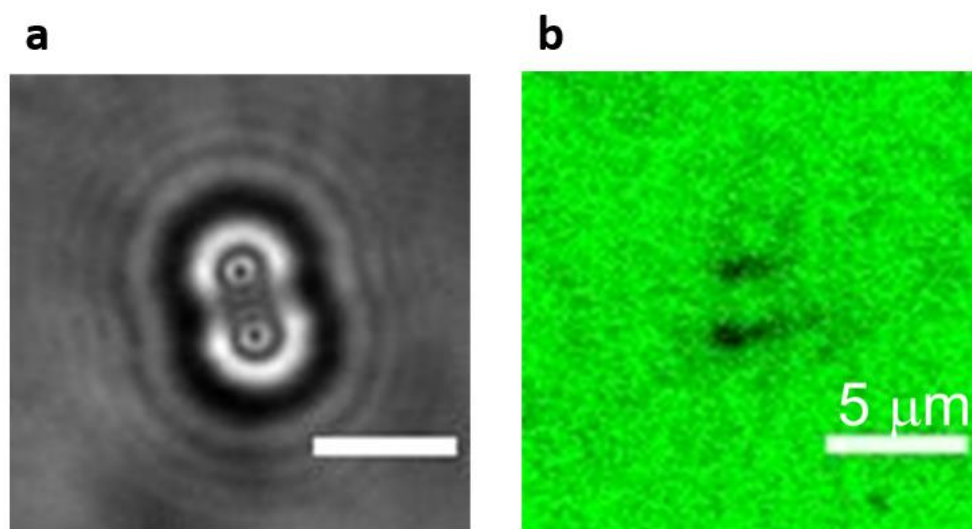


Figure 14. Depletion tracks of a dimer after 15 minutes from enzyme addition. a) bright field micromotor. **b)** FAM depletion track under FITC channel on the same region.

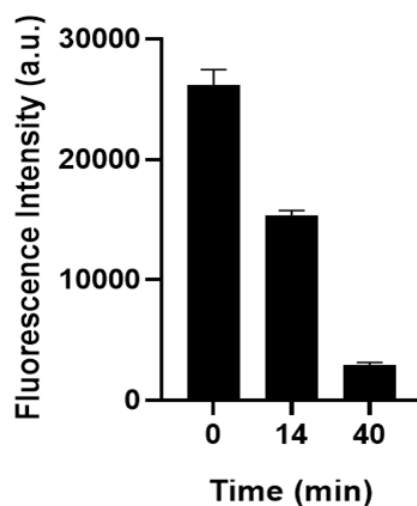


Figure 15. Fluorescence intensity of randomly chosen unvisited regions on the surface at different time after reaction.

3.3 Assembling DNA fuels on glass surface

A glass surface was used in place of a gold surface such that all the thiol-gold bonds from the system were eliminated to avoid DTT-mediated DNA dissociation from the surface. In order to optimize the activity of Exonuclease III, 1 mM DTT was added to the surface to better stabilize the enzyme. Two additives were also added in the surface solution to accelerate the DNA motor. First, formamide was added to the surface solution as Bazrafshan et al. showed that formamide increases the net displacement of DNA motor by increasing the hydrolysis rate of enzyme.⁷ Triton X was also added to reduce DNA nonspecifically bound to the surface.

5-micron silica beads coated with particle guide DNA were hybridized to the glass surface presenting complementary DNA strands. The particles were immobile on the surface until Exonuclease III addition. At one minute after the addition of enzyme, there was a depletion spot underneath every pictured particle on the FAM-labelled surface, indicating

the occurrence of hydrolysis at the surface-particle junction. After 100 units of Exonuclease III were added to the surface, several 15-minute time-lapse videos on several regions of interests revealed the motor translocation across the surface. Multiple $\sim 10 \mu\text{m}$ consecutive depletion tracks representing the loss of FAM-labelled DNA fuel strands were observed under the particles (**Figure 16 and Figure 17a**).

In order to obtain longer depletion tracks, the same reaction was repeated with longer reaction time. After 30 minutes of the reaction, multiple depletion tracks with $\sim 20 \mu\text{m}$ consecutive depletion tracks were observed (**Figure 17b**). The Exonuclease III-powered motor travelled in a processive way within the first 30 minutes of reaction.

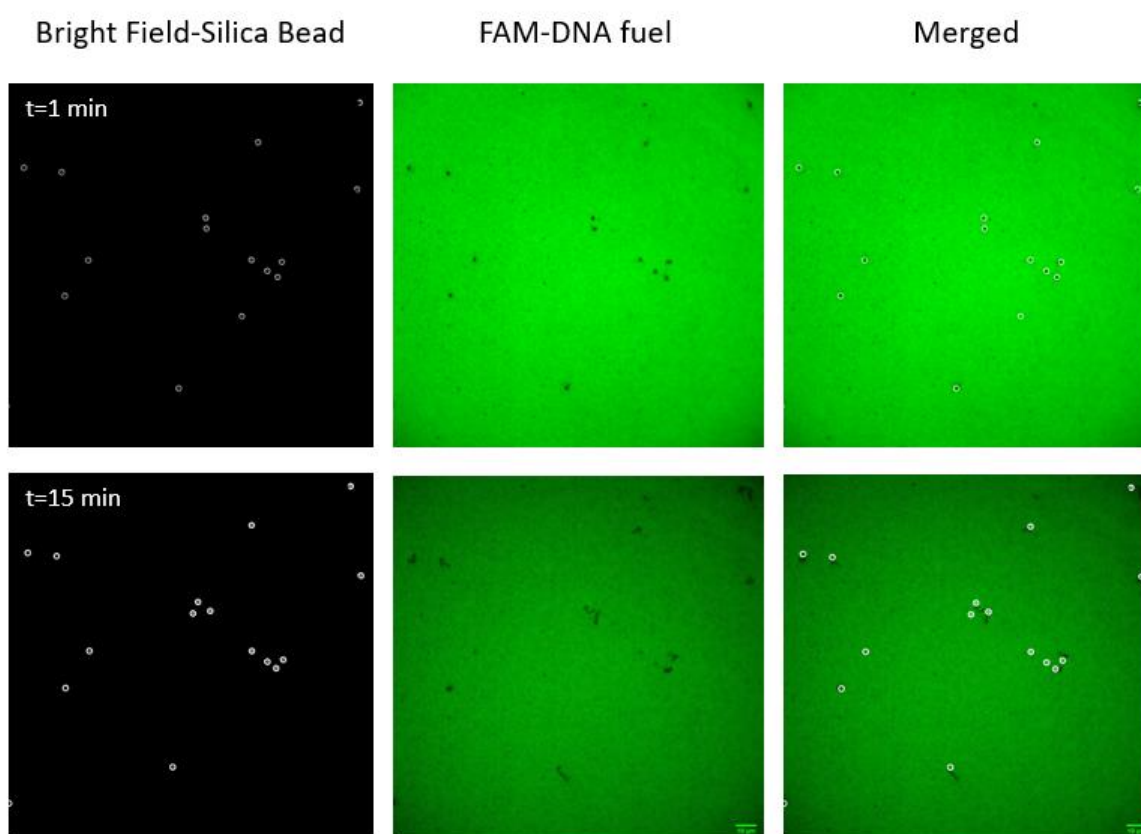


Figure 16. Time-lapse fluorescence image of Bright Field Silica bead, FAM-DNA fuel, and merged image of DNA motors. $10 \mu\text{m}$ depletion tracks were observed 15 minutes after the addition of 100 units of Exonuclease III.

However, in some regions on the surface, the motors headed towards the same direction. This translocation pattern was observed in the merged images of bright field silica beads and FAM-DNA fuels after both the 15-minute reaction and the 30-minute reaction (**Figure 17**). The microfluid flow within the IBIDI chambers may contribute to the unidirectionality of the motor. The DNA fuel can only form a 10-basepair duplex with the particle guide DNA. Therefore, the melting temperature (T_m) of the duplex is low. As a result, the driving force attributed to DNA hybridization is relatively weak and shearing force loaded on the particle at the beginning by the liquid flow is predominant in controlling the direction of motion.

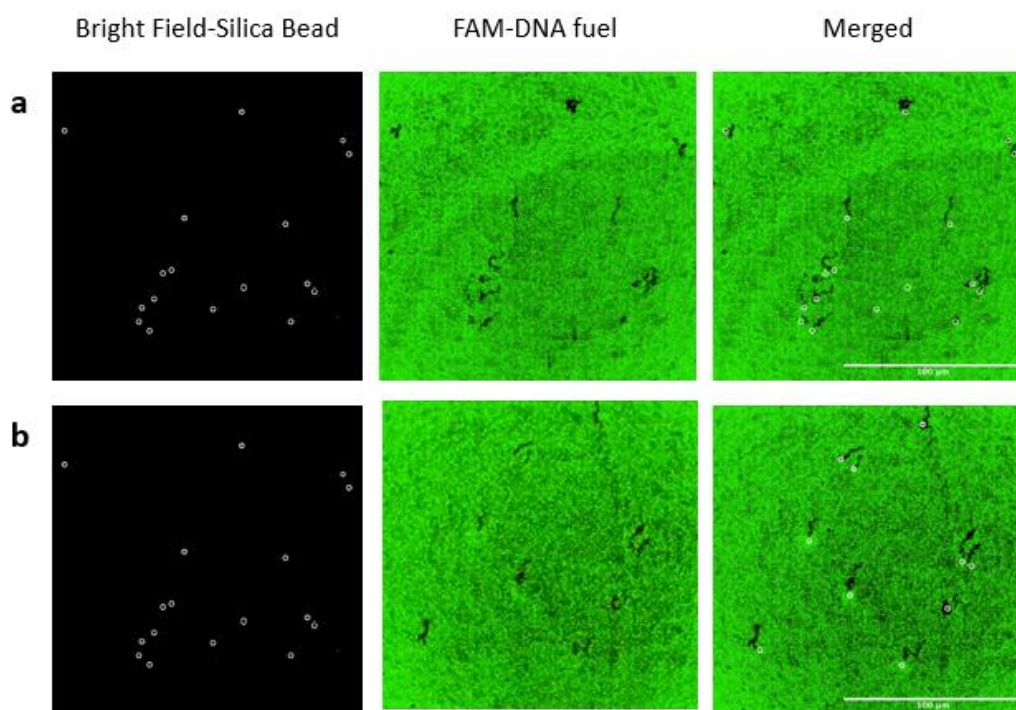


Figure 17. Tracks showing particles moved in the same direction after a) 15-minute reaction and b) 30-minute reaction. All the motors were heading downwards in the Merged image.

In principle, particles translocate on the surface by avoiding the consumed DNA fuel and randomly heading towards regions with available fuels. To improve the T_m of DNA duplex formed by the DNA fuel and particle DNA, 1x Exonuclease III buffer was substituted with 1x RNase H buffer (3 mM $MgCl_2$, 50 mM Tris-HCl, pH = 8.3) which has a high concentration of divalent cation. After the concentration of magnesium cation was increased to 3 mM, depletion tracks after a 30-minute reaction revealed that motors were capable to move in different directions (**Figure 18**).

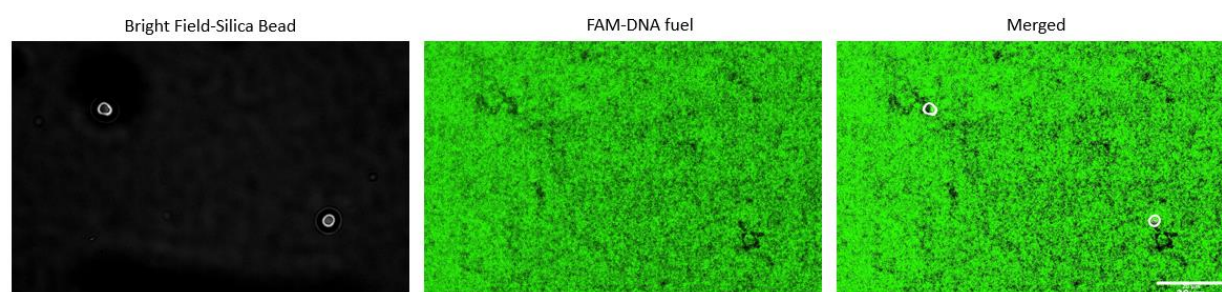
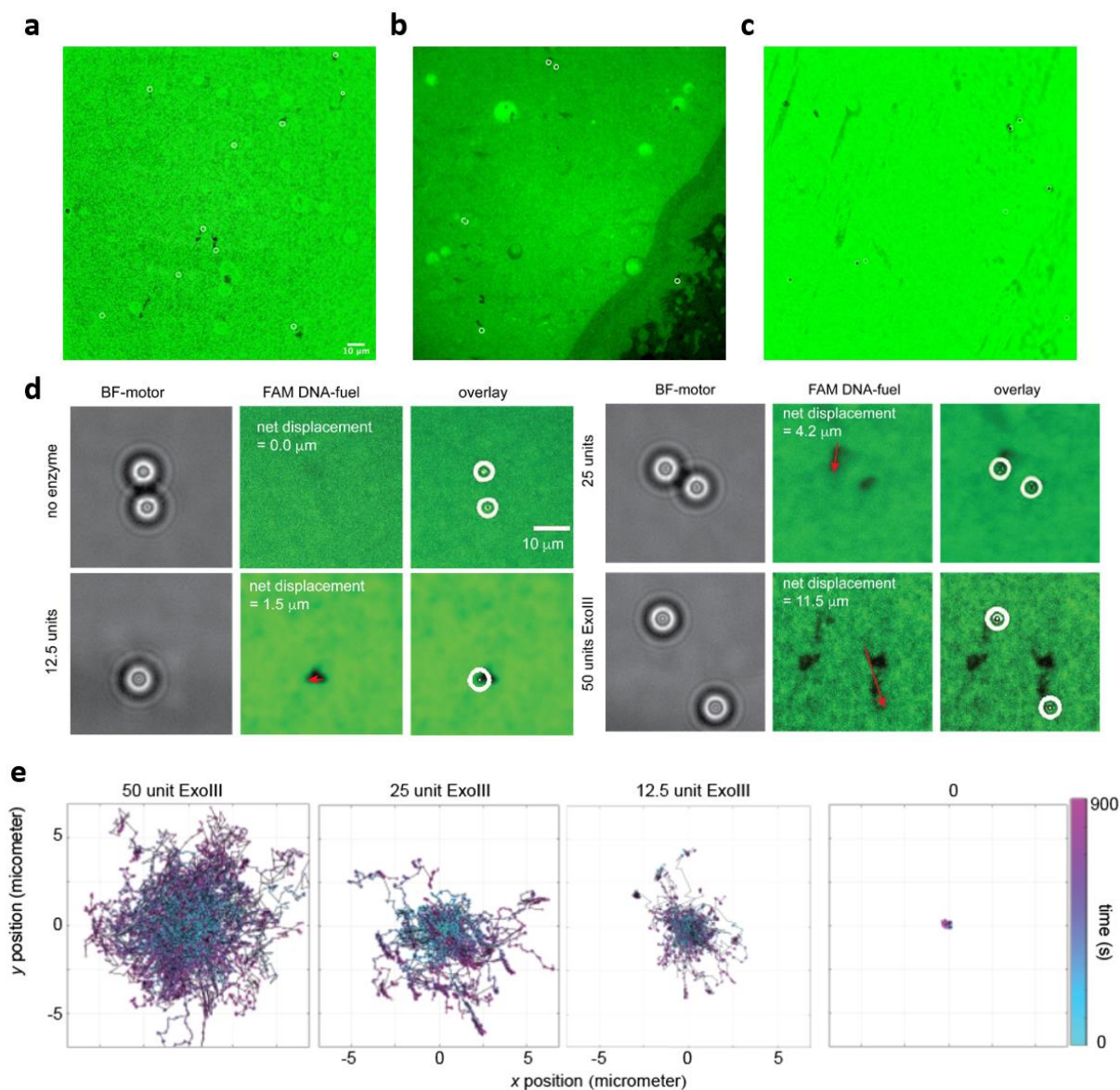


Figure 18. Particles moved in different direction under high magnesium concentration. In the merged image, the motor on the left had moved to its right, while the motor on the right had moved upwards.

Since it was noticed that some particles dissociated during the 15-minute and 30-minute reaction, and the surface degraded fast within 15 minutes of reaction, reactions at lower Exonuclease III concentrations were performed to reduce the background hydrolysis. Some depletion tracks after 15 minutes with the addition of 50, 25, 12.5 units of Exonuclease III was shown in **Figure 19a, b, and c**, respectively. Track analysis and trajectory analysis results showed that motor traveled further and had higher net displacement under higher enzyme concentration (**Figure 19d, e, f**). When no enzyme was added to the surface, the particle remained stalled to the surface for 15 minutes,

which confirmed that the motions of the particles were enzyme driven. Diffusion type of the particles were also assessed by calculating the anomalous diffusion exponent α . There is a group of motor with $\alpha > 1$ at every enzyme concentration, revealing that some of the particles were diffusing superdiffusively on the surface regardless of enzyme concentration in solution over 30 minutes (**Figure 19g**).



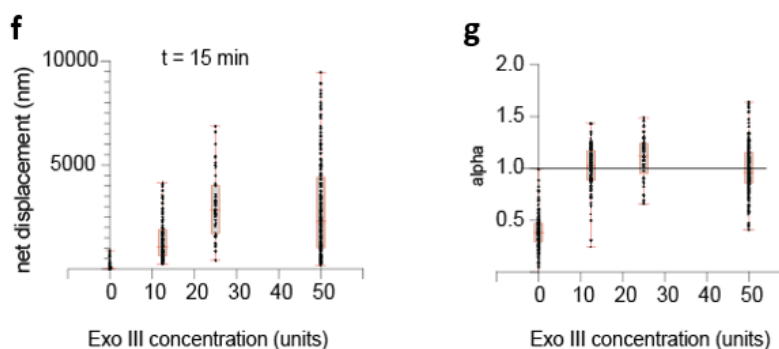


Figure 19. Tracks and trajectory analysis for reactions with lower enzyme concentration. a) Depletion tracks captured after 30 minutes of reaction under 50 b) 25 c) 12.5 units of Exonuclease III on the surface. d) end to end distance of representative depletion tracks under various enzyme concentrations. e) Ensemble of different trajectories under different enzyme concentrations. f) Plots of net displacement and g) alpha values for motors translocate under various Exonuclease III concentration.

Lastly, the decrease in surface intensity triggered by Exonuclease III was investigated. Upon the addition of 12.5 units of enzyme, ~50% of the surface intensity was lost after 15 minutes (**Figure 20a**). In the presence of 50 units of enzyme, the FAM intensity of the surface decreased most quickly in the first 15 minutes (**Figure 20b**). When 100 units of Exonuclease III were added to the surface, the surface completely degraded after 15 minutes. The loss of FAM fluorescence intensity on the surface could be attributed to the nonspecific reactivity of Exonuclease III, which was further studied using DNA-coated gold nanoparticle assays.

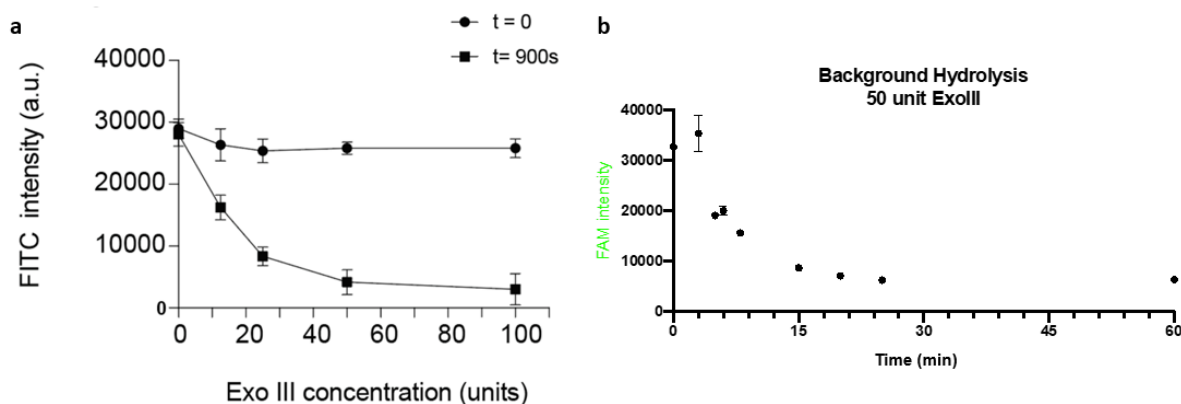


Figure 20. Degradation of FAM-labelled surface a) 15 minutes after various concentrations of enzyme were added and b) 60 minutes after 50 units of Exonuclease III were added.

3.4 Fluorescence-based kinetic assay for Exonuclease III activity

The development of SNA by Mirkin et al.²⁸ has catalyzed the interest from the world in their application in nanomotor design due to its high programmability and unique properties. SNAs are versatile in applications due to their ease of functionalization and tunable dimensions such as size of the nanoparticles, DNA sequences and modifications. SNA also exhibits a series of distinct properties from free oligonucleotides and nanoparticles, including the enhancement of nucleases activities. Qu et al. reported the high activity of Exonuclease III towards SNA as compared to free DNA, which suggested the high processivity of Exonuclease III for SNAs.¹⁹ Therefore, in this study, DNA-coated gold nanoparticles were used to assess the kinetics and activity of Exonuclease III while exploring the optimal experimental condition both in solution and on a glass surface. The DNA monolayer on surface was reproduced in the gold nanoparticle assay through the design shown in **Figure 21**: gold nanoparticles were functionalized with DNA anchor

strands hybridizing to DNA fuel strands. A FAM fluorophore at the 3' end of the fuel strand was used as a probe to detect enzymatic cleavage.

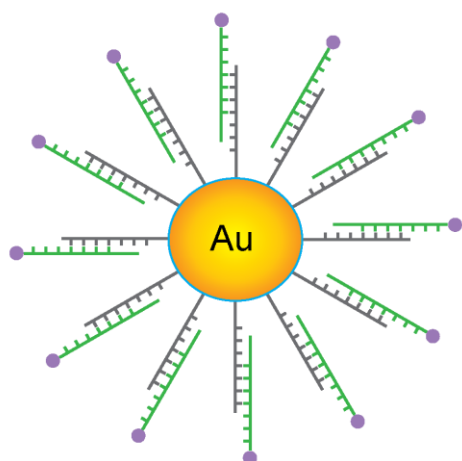


Figure 21. Proposed schematic design of DNA-labelled gold nanoparticle. The gold nanoparticle is labeled in yellow, the anchor strands are labelled in grey, and the DNA fuel strands are labelled in green. The FAM fluorophores are shown as purple circles.

3.4.1 Quantification of DNA loading density and quenching efficiency

SNAs are resistant to the degradation of nuclease when the oligonucleotides labelled on the nanoparticle are too dense, which resists nuclease binding due to steric hindrance.²⁹ The number of oligonucleotides coated on gold nanoparticles is tuned by varying the amount of DNA fuel strands hybridized to the DNA anchor functionalized on the gold nanoparticle. Therefore, before exploring the interactions between Exonuclease III and oligonucleotide-coated gold nanoparticles, the loading density of oligonucleotides on gold nanoparticles was optimized and quantified.

After oligonucleotides were functionalized to gold nanoparticles, DTT was added to liberate the thiolated oligonucleotides from gold nanoparticle following the reaction shown in **Figure 22**. The amount of DNA release was quantified using a calibration curve by measuring the fluorescence intensity of known concentrations of DNA fuels under identical conditions (**Figure 23a**). When preparing calibration curves, the sample of DNA fuels and gold nanoparticles after DTT addition was reproduced by mixing DNA fuel strand with gold nanoparticles labelled with poly-T strands. The concentration of DNA fuel strand in sample was calculated from the calibration curve. The loading density of gold nanoparticle constructed using different amounts of DNA fuels was obtained by dividing the calculated DNA fuel concentration by gold nanoparticle concentration (**Figure 23b**). When 0.5 nmol of DNA fuel was added, there were 77 strands on each gold nanoparticle, which matched the expected value.³⁰

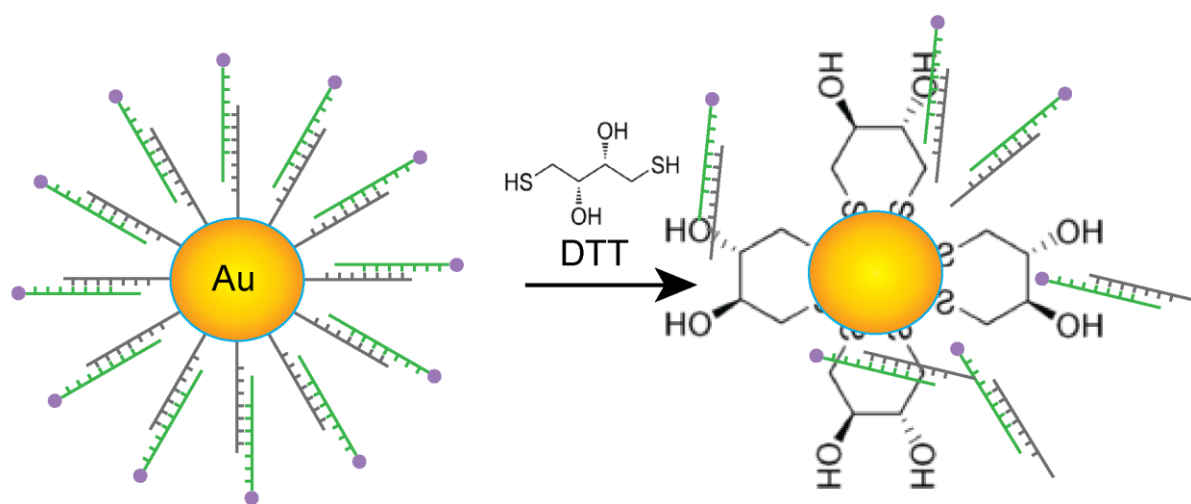


Figure 22. *DTT degrades the DNA functionalized gold nanoparticle through thiol displacement.*

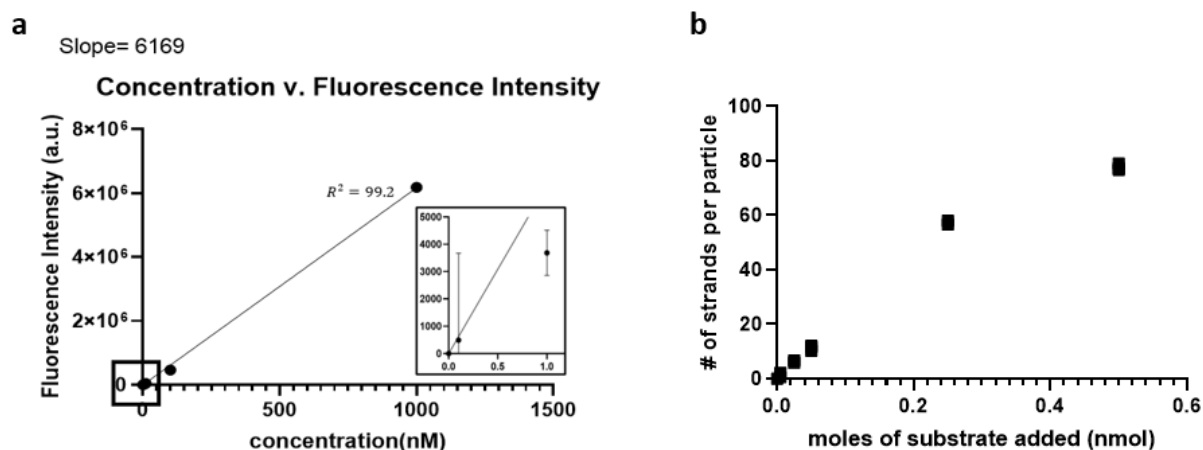


Figure 23. Quantification of DNA fuel strands coated on the gold nanoparticle. a) Calibration between free DNA fuel and gold nanoparticle labelled with noncomplementary DNA. b) Number of strands per particle when hybridized to various amounts of DNA fuel strands.

The nanometal surface energy transfer (NSET) rate and the radiative lifetime of fluorophores are changed when placed in adjacent to metal particles.³¹ Gold nanoparticles are claimed to exhibit efficient fluorescence quenching via gold-fluorophore interactions.³² To investigate the detection ability of the gold nanoparticle assays as fluorescence-based probes, the quenching efficiency of gold nanoparticle assays was investigated.

The gold nanoparticle assay used in this study was designed where the FAM fluorophore-labelled DNA fuel hybridized to the oligonucleotide on the nanoparticle. Dissociation of fuel strand released the FAM from the particle surface, dequenching the fluorescence (**Figure 24**). The quenching efficiency was calculated by subtracting the ratio of fluorescence intensity of bounded DNA fuel to fluorescence intensity of released DNA fuel from 1. Approximately 50% quenching efficiency was achieved when 0.5 and 0.25

nmols of DNA fuel was added. Based on the results above, it can be concluded that DNA-coated gold nanoparticle is a feasible assay used to test enzyme activity.

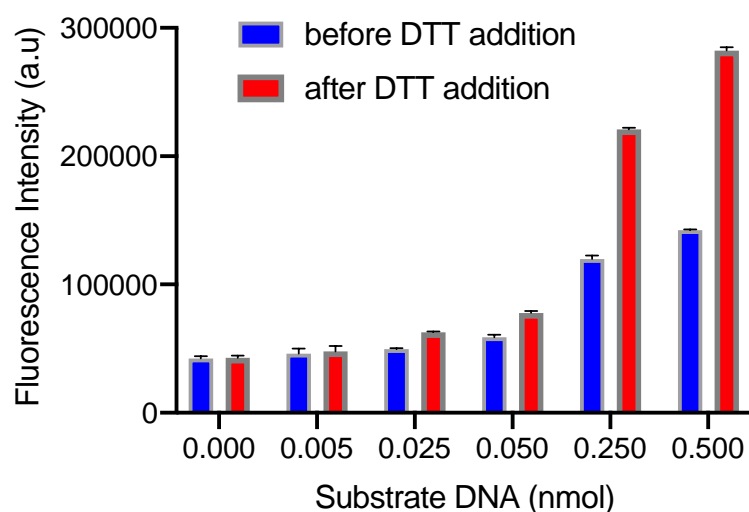


Figure 24. Separation of fluorophores and gold nanoparticle leads to a fluorescence increase.

3.4.2 Specificity and reactivity of Exonuclease III

After the loading density and quenching efficiency of DNA-coated gold nanoparticles were confirmed, the specificity and reactivity of Exonuclease III towards the blunt 3' end were tested using the gold nanoparticle assay. In order to have the Exonuclease III-powered motor to function, Exonuclease III has to specifically cleave the 3' end of the fuel once it is attached to a DNA leg while not cleave any single-stranded 3' end. Introduction of guide DNA generates blunt 3' end site at the DNA fuel on the DNA Anchor-coated gold nanoparticles. Exonuclease III is expected to recognize the cleavage site and initiate hydrolysis at the 3' terminus of DNA fuel (**Figure 25a**). In contrast, when only the DNA fuel hybridizes to the anchor strand attached to the gold nanoparticle (**Figure 25b**), there is no blunt 3' end present and no cleavage by Exonuclease III is expected. The enzyme

cleavage is going to be followed by fluorophore release from gold nanoparticles, resulting in an increase in fluorescence signal. To maintain Exonuclease III activity, 10 μ M DTT was added to the reaction despite dissociation of anchored DNA resulted.

The cleavage activity of Exonuclease III was real-time monitored by fluorescence measurement shown in **Figure 26**. When 1 unit of Exonuclease III was added to 0.5 nM of DNA-functionalized gold nanoparticles, both the specific and nonspecific reaction took place so rapidly that the reactions in the first few seconds was not captured. The specific reaction was faster than the non-specific reaction in the first five minutes, while the reaction in both assays reached saturation point after 10 minutes. Therefore, lower enzyme concentrations were tested to find the optimal enzyme-to-substrate ratio to suppress the non-specific reaction and decelerate Exonuclease III cleavage rate.

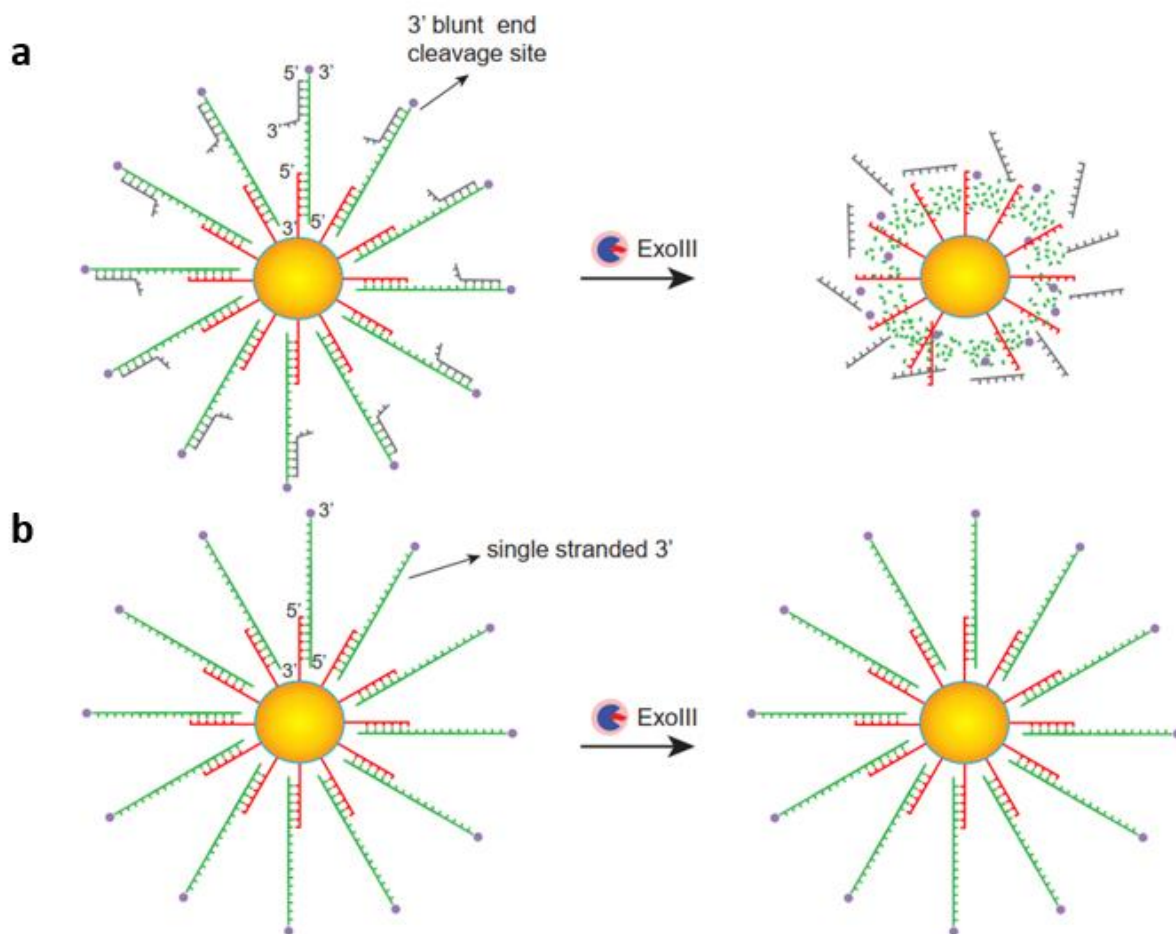


Figure 25. Schematic for AuNP assays used to test Exonuclease III specificity. a) Specific cleavage assay. Particle guide DNA are hybridized to the DNA fuel, creating a blunt 3' end at the DNA fuel. An increase in fluorescence intensity after adding Exonuclease III is expected. b) Nonspecific cleavage assay. DNA fuel strands with a fluorophore on their 3' ends are attached to the anchor strands coated on the gold nanoparticle. There is no blunt 3' end in this assay, and no change in fluorescence intensity after enzyme addition is expected. In the above illustrations, gold nanoparticles are shown in yellow spherical particles. Anchor strands are labelled in red, DNA fuel strands are labelled in green, and particle guide DNAs are labelled in grey.

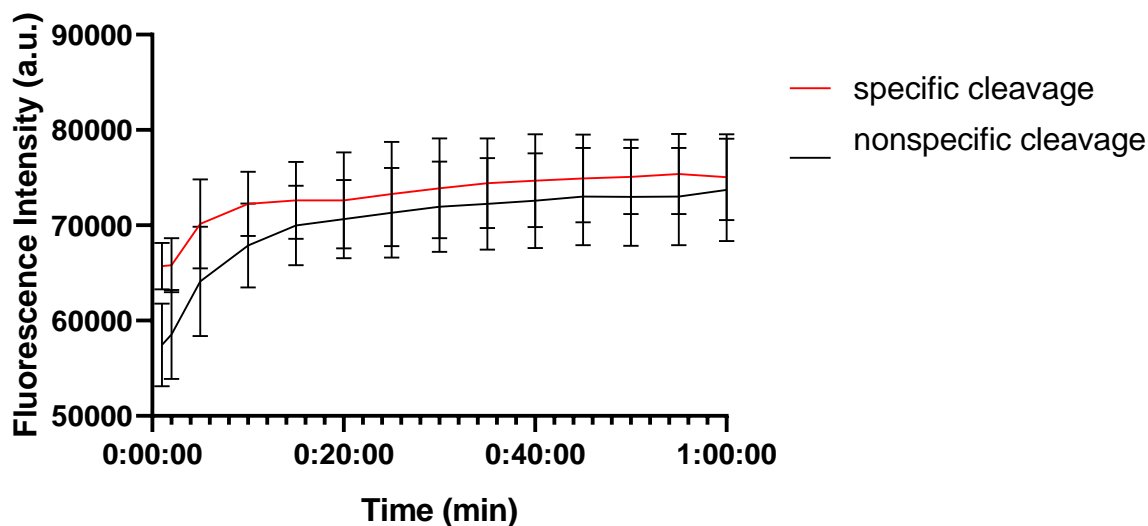


Figure 26. Exonuclease III kinetics measurement for 1 hour on fluorescence intensity after the addition of 1 unit Exonuclease III.

0.5, 0.1, 0.05, and 0.01 unit of Exonuclease III was added to 0.5 nM DNA-coated gold nanoparticle, and the kinetics measurements were shown in **Figure 27**. The cleavage rates of Exonuclease III on both specific and nonspecific assays were tuned down by decreasing the enzyme concentration. The reactions in both assays were completed after 40 minutes. The suppression of nonspecific cleavage was also notable at lower enzyme concentrations. After 0.5 unit of Exonuclease III was added to the reaction, nonspecific cleavage was restrained. Less DNA fuel was cleaved nonspecifically after 40 minutes (**Figure 28**). Similar conclusion can be drawn from the data obtained when 0.25 unit of Exonuclease III was added. Nevertheless, the kinetic results confirmed that there was a significant off-target effect of Exonuclease III towards single-stranded DNA with a 3' end exposed.

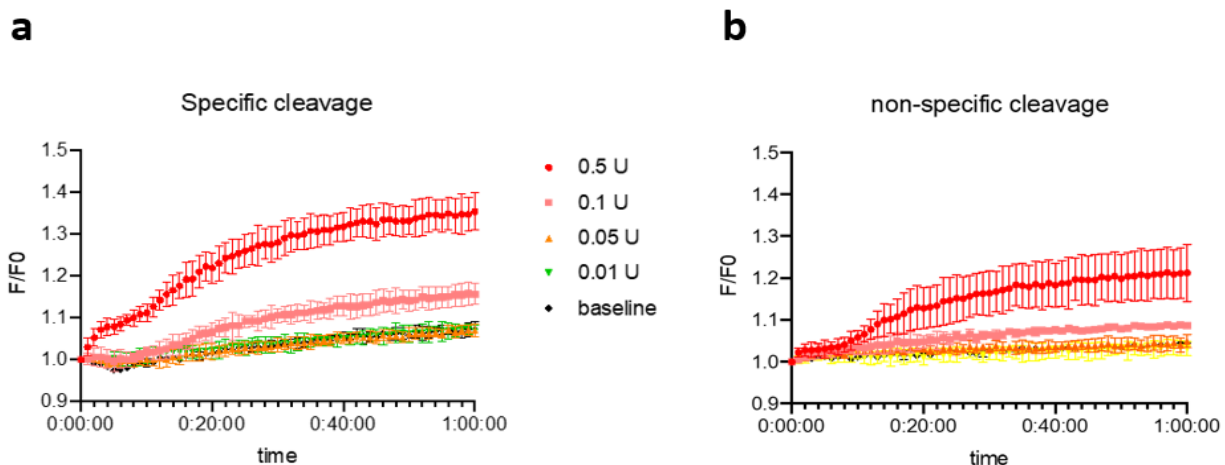


Figure 27. Exonuclease III kinetics measurement for 1 hour on fluorescence intensity at lower enzyme concentrations.

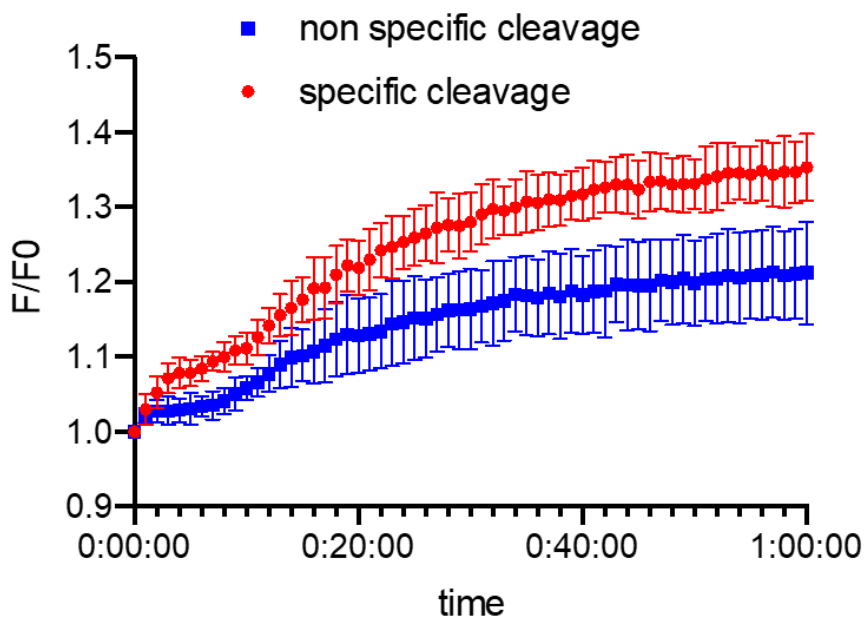


Figure 28. Comparison between 1-hr specific cleavage and nonspecific cleavage under 0.5 unit of Exonuclease III.

Notably, a drop followed by subsequent increase of fluorescence intensity in kinetic measurement plots for specific cleavage was observed at all enzyme concentrations (**Figure 27a**). This feature was also detected by Hsiao et al. and referred to as “target stacking”.³³ When DNA fuels are hybridized to the anchors labelled on the gold nanoparticles, some of the DNA fuel strands remain unhybridized in solution. As Exonuclease III removes nucleotides from the gold nanoparticles, more and more anchor strands are exposed. The free DNA fuels in solution hybridize to the unoccupied anchor strands and get quenched, leading to a decrease in fluorescence intensity. As the reaction proceeds, all the free DNA fuels in solution bind to unoccupied anchor strands. Exonuclease III continues to cleave all the bound DNA fuels, leading to an increase following the initial drop in fluorescence intensity.

4. Conclusions

It was suggested from the above experiments that Exonuclease III has the potential to be used as a catalyst to power the motion of DNA-based rolling motor on DNA-coated surface. The Exonuclease III-powered DNA motors demonstrate random superdiffusive motion and are capable of translocating over 20 μm within 30 minutes.

The nonspecific activity of Exonuclease III was also noticed and was accountable for the fast background hydrolysis observed in surface experiments. The “target stacking” interaction between free DNA fuel and oligonucleotides observed on gold nanoparticle experiments could brake the activity of Exonuclease III on surface-particle junction. We recognize several tunable parameters to increase the processivity and speed of this motor. First, the properties of oligonucleotide can be optimized. For example, more nucleotides

can be added to the 3' end of the particle DNA to protect the DNA leg from being nonspecifically cleaved by Exonuclease III. Similarly, the DNA fuel can be lengthened so that the 3' overhang would be more differentiable from a blunt 3' end by Exonuclease III. Base-pair mismatches can be introduced at different positions to tune reaction speeds in the system.³⁴ In addition, a photostable fluorophore such as Cy3B can be adopted in the system in place of FAM to prevent photobleaching. We anticipate future experimental work to explore these parameters and improve the current system on DNA rolling motor.

Next, alternative enzymes can be used to power the DNA-based rolling system on DNA tracks. N.BbvC IB is a restriction endonuclease that can recognize a 7-base pair sequence in a DNA duplex and introduce a nick at precisely determined position by cleaving one DNA strand. This enzyme was used to design a DNA motor that moves on a DNA track.⁹ Nt.BspQI is also a candidate as motion-powering enzyme. It is also a nicking endonuclease that recognizes a specific sequences of DNA duplex and cleaves only one DNA strand with the other one intact.

Furthermore, besides enzyme-powered rolling motor, it is also desirable to develop a rolling motor powered by enzyme-free reaction. Zhang et al. developed an entropy-driven autocatalytic system based on nucleic acid toehold-mediated strand displacement, in which the input of an oligonucleotides catalyzes the release of a certain oligonucleotide that in turn catalyzes reactions in the following steps.³⁵ This reaction can be used to power rolling motion of catalyst strand-coated particle on DNA-labelled surface. The schematic of reaction pathway is shown in **Figure 29**.

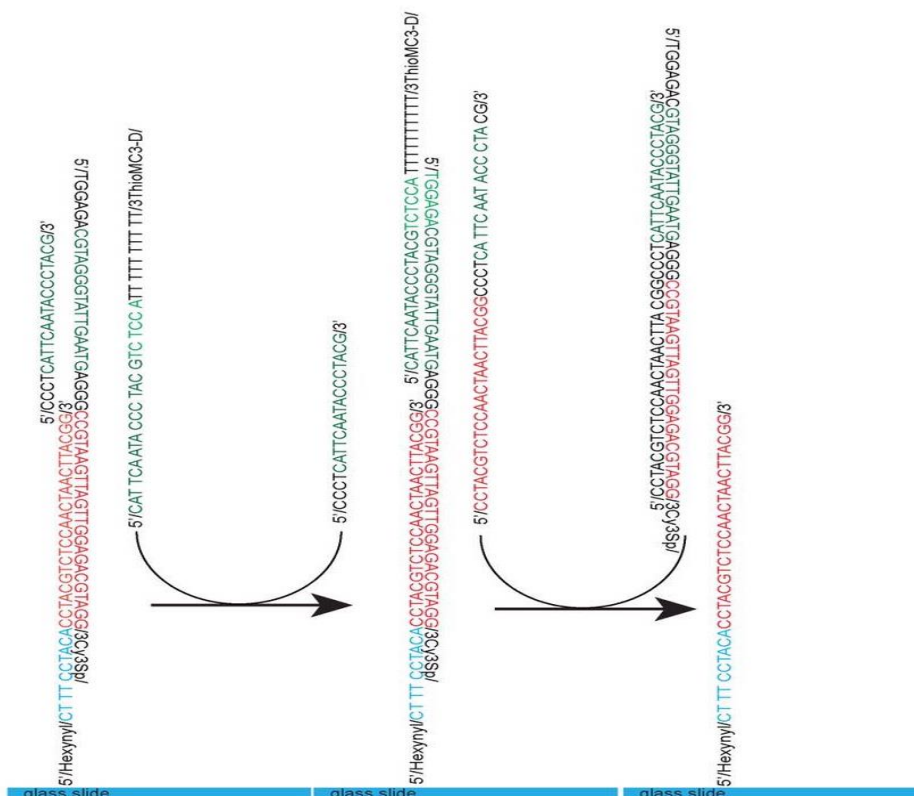


Figure 29. Schematic design for DNA rolling motor powered by toehold-mediated strand displacement reactions. The anchor strand is coated on the glass surface with the substrate strand hybridizing to the anchor strand. A blocker strand is hybridized to the substrate until the addition of catalyst strand, which releases the blocker strand from the substrate and hybridizes to the substrate instead. After the fuel strand was added, the substrate dissociates from the anchor strand and leaves the surface hybridizing to the fuel strand. The particles are labelled with catalyst strands. When the particles are released to the surface, the blocker strands are removed. The switch of the rolling system can be turned on by introducing the fuel strand to the surface, which would remove catalyst-bound substrate from the surface. Complementary domains are shown in the same color.

With the sensitivity of this DNA-based rolling motor system improved, it could be applied in the field of DNA-based sensing. Without the limitation brought by RNA tracks, the DNA-based system would become a new assay in label-free sensing in the clinical field.

5. References

1. von Delius, M.; Leigh, D. A., Walking molecules. *Chemical Society Reviews* **2011**, *40* (7), 3656-3676.
2. Woehlke, G.; Schliwa, M., Walking on two heads: the many talents of kinesin. *Nature Reviews Molecular Cell Biology* **2000**, *1* (1), 50-58.
3. Shao, J.; Cao, S.; Williams, D. S.; Abdelmohsen, L. K. E. A.; van Hest, J. C. M., Photoactivated Polymersome Nanomotors: Traversing Biological Barriers. **2020**, *59* (39), 16918-16925.
4. Ren, L.; Wang, W.; Mallouk, T. E., Two Forces Are Better than One: Combining Chemical and Acoustic Propulsion for Enhanced Micromotor Functionality. *Accounts of Chemical Research* **2018**, *51* (9), 1948-1956.
5. Zhou, D.; Ren, L.; Li, Y. C.; Xu, P.; Gao, Y.; Zhang, G.; Wang, W.; Mallouk, T. E.; Li, L., Visible light-driven, magnetically steerable gold/iron oxide nanomotors. *Chemical Communications* **2017**, *53* (83), 11465-11468.
6. Yehl, K.; Mugler, A.; Vivek, S.; Liu, Y.; Zhang, Y.; Fan, M.; Weeks, E. R.; Salaita, K., High-speed DNA-based rolling motors powered by RNase H. *Nature Nanotechnology* **2016**, *11* (2), 184-190.
7. Bazrafshan, A.; Meyer, T. A.; Su, H.; Brockman, J. M.; Blanchard, A. T.; Piranej, S.; Duan, Y.; Ke, Y.; Salaita, K., Tunable DNA Origami Motors Translocate Ballistically Over μm Distances at nm/s Speeds. **2020**, *59* (24), 9514-9521.
8. Yin, P.; Yan, H.; Daniell, X. G.; Turberfield, A. J.; Reif, J. H., A Unidirectional DNA Walker That Moves Autonomously along a Track. **2004**, *43* (37), 4906-4911.

9. Bath, J.; Green, S. J.; Turberfield, A. J., A Free-Running DNA Motor Powered by a Nicking Enzyme. **2005**, *44* (28), 4358-4361.
10. Davey, S. G., Roll this way. *Nature Reviews Chemistry* **2020**, *4* (4), 169-169.
11. Jung, C.; Allen, P. B.; Ellington, A. D., A stochastic DNA walker that traverses a microparticle surface. *Nature nanotechnology* **2016**, *11* (2), 157-163.
12. Yao, D.; Bhadra, S.; Xiong, E.; Liang, H.; Ellington, A. D.; Jung, C., Dynamic Programming of a DNA Walker Controlled by Protons. *ACS Nano* **2020**, *14* (4), 4007-4013.
13. Pei, R.; Taylor, S. K.; Stefanovic, D.; Rudchenko, S.; Mitchell, T. E.; Stojanovic, M. N., Behavior of Polycatalytic Assemblies in a Substrate-Displaying Matrix. *Journal of the American Chemical Society* **2006**, *128* (39), 12693-12699.
14. Cha, T.-G.; Pan, J.; Chen, H.; Salgado, J.; Li, X.; Mao, C.; Choi, J. H., A synthetic DNA motor that transports nanoparticles along carbon nanotubes. *Nature Nanotechnology* **2014**, *9* (1), 39-43.
15. Allentoft, M. E.; Collins, M.; Harker, D.; Haile, J.; Oskam, C. L.; Hale, M. L.; Campos, P. F.; Samaniego, J. A.; Gilbert, M. T. P.; Willerslev, E.; Zhang, G.; Scofield, R. P.; Holdaway, R. N.; Bunce, M., The half-life of DNA in bone: measuring decay kinetics in 158 dated fossils. **2012**, *279* (1748), 4724-4733.
16. Linxweiler, W.; Hörz, W., Sequence specificity of exonuclease III from *E. coli*. *Nucleic Acids Res* **1982**, *10* (16), 4845-4859.
17. Mol, C. D.; Kuo, C.-F.; Thayer, M. M.; Cunningham, R. P.; Tainer, J. A., Structure and function of the multifunctional DNA-repair enzyme exonuclease III. *Nature* **1995**, *374* (6520), 381-386.

18. Luo, M.; Xuan, M.; Huo, S.; Fan, J.; Chakraborty, G.; Wang, Y.; Zhao, H.; Herrmann, A.; Zheng, L., Four-Dimensional Deoxyribonucleic Acid–Gold Nanoparticle Assemblies. **2020**, *59* (39), 17250-17255.
19. Qu, X.; Zhu, D.; Yao, G.; Su, S.; Chao, J.; Liu, H.; Zuo, X.; Wang, L.; Shi, J.; Wang, L.; Huang, W.; Pei, H.; Fan, C., An Exonuclease III-Powered, On-Particle Stochastic DNA Walker. **2017**, *56* (7), 1855-1858.
20. Lee, H. J.; Li, Y.; Wark, A. W.; Corn, R. M., Enzymatically Amplified Surface Plasmon Resonance Imaging Detection of DNA by Exonuclease III Digestion of DNA Microarrays. *Analytical Chemistry* **2005**, *77* (16), 5096-5100.
21. Blanchard, A. T.; Bazrafshan, A. S.; Yi, J.; Eisman, J. T.; Yehl, K. M.; Bian, T.; Mugler, A.; Salaita, K., Highly Polyvalent DNA Motors Generate 100+ pN of Force via Autochemophoresis. *Nano Letters* **2019**, *19* (10), 6977-6986.
22. Zhang, Y.; Ge, C.; Zhu, C.; Salaita, K., DNA-based digital tension probes reveal integrin forces during early cell adhesion. *Nature Communications* **2014**, *5* (1), 5167.
23. Sbalzarini, I. F.; Koumoutsakos, P., Feature point tracking and trajectory analysis for video imaging in cell biology. *Journal of structural biology* **2005**, *151* (2), 182-195.
24. Panchuk-Voloshina, N.; Haugland, R. P.; Bishop-Stewart, J.; Bhalgat, M. K.; Millard, P. J.; Mao, F.; Leung, W.-Y.; Haugland, R. P., Alexa Dyes, a Series of New Fluorescent Dyes that Yield Exceptionally Bright, Photostable Conjugates. **1999**, *47* (9), 1179-1188.
25. Fjelstrup, S.; Andersen, M. B.; Thomsen, J.; Wang, J.; Stougaard, M.; Pedersen, F. S.; Ho, Y.-P.; Hede, M. S.; Knudsen, B. R., The Effects of Dithiothreitol on DNA. *Sensors (Basel)* **2017**, *17* (6), 1201.

26. Zhang, L.; Wang, Z.-X.; Liang, R.-P.; Qiu, J.-D., Easy Design of Colorimetric Logic Gates Based on Nonnatural Base Pairing and Controlled Assembly of Gold Nanoparticles. *Langmuir* **2013**, *29* (28), 8929-8935.
27. Thaxton, C. S.; Hill, H. D.; Georganopoulou, D. G.; Stoeva, S. I.; Mirkin, C. A., A Bio-Bar-Code Assay Based upon Dithiothreitol-Induced Oligonucleotide Release. *Analytical Chemistry* **2005**, *77* (24), 8174-8178.
28. Mirkin, C. A.; Letsinger, R. L.; Mucic, R. C.; Storhoff, J. J., A DNA-based method for rationally assembling nanoparticles into macroscopic materials. *Nature* **1996**, *382* (6592), 607-9.
29. Prigodich, A. E.; Alhasan, A. H.; Mirkin, C. A., Selective enhancement of nucleases by polyvalent DNA-functionalized gold nanoparticles. *J Am Chem Soc* **2011**, *133* (7), 2120-3.
30. Hurst, S. J.; Lytton-Jean, A. K. R.; Mirkin, C. A., Maximizing DNA loading on a range of gold nanoparticle sizes. *Analytical chemistry* **2006**, *78* (24), 8313-8318.
31. Swierczewska, M.; Lee, S.; Chen, X., The design and application of fluorophore-gold nanoparticle activatable probes. *Phys Chem Chem Phys* **2011**, *13* (21), 9929-9941.
32. Xu, J.-J.; Zhao, W.-W.; Song, S.; Fan, C.; Chen, H.-Y., Functional nanoprobe for ultrasensitive detection of biomolecules: an update. *Chemical Society Reviews* **2014**, *43* (5), 1601-1611.
33. Hsiao, J. C.; Buryska, T.; Kim, E.; Howes, P. D.; deMello, A. J., Tuning DNA-nanoparticle conjugate properties allows modulation of nuclease activity. *Nanoscale* **2021**, *13* (9), 4956-4970.

34. Irmisch, P.; Ouldridge, T. E.; Seidel, R., Modeling DNA-Strand Displacement Reactions in the Presence of Base-Pair Mismatches. *Journal of the American Chemical Society* **2020**, *142* (26), 11451-11463.
35. Zhang, D. Y.; Turberfield, A. J.; Yurke, B.; Winfree, E., Engineering Entropy-Driven Reactions and Networks Catalyzed by DNA. **2007**, *318* (5853), 1121-1125.